Structure and properties of Na5FeSi4O12 crystallized from 5Na2O–Fe2O3–8SiO2 glass

AHMADZADEH, M, OLDS, TA, SCRIMSHIRE, Alex <http://orcid.org/0000-0002-6828-3620>, BINGHAM, Paul <http://orcid.org/0000-0001-6017-0798> and MCCLOY, JS

Published version

AHMADZADEH, M, OLDS, TA, SCRIMSHIRE, Alex, BINGHAM, Paul and MCCLOY, JS (2018). Structure and properties of Na5FeSi4O12 crystallized from 5Na2O–Fe2O3–8SiO2 glass. Acta Crystallographica Section C: Structural Chemistry, 74 (12), 1595-1602.

research paper

Acta Cryst C STRUCTURAL CHEMISTRY

ISSN 2053-2296

Structure and properties of $Na_5FeSi_4O_{12}$ crystallized from $5Na_2O–Fe_2O_3–8SiO_2$ glass

Mostafa Ahmadzadeh,[a] Travis A. Olds,[a] Alex Scrimshire,[b] Paul A. Bingham[b] and John S. McCloy[a]*

[a]School of Mechanical and Materials Engineering, Washington State University, Pullman, Washington 99164, USA, and [b]Materials and Engineering Research Institute, Sheffield Hallam University, Sheffield S1 1WB, England. *Correspondence e-mail: john.mccloy@wsu.edu

Received 21 September 2018
Accepted 11 October 2018

Edited by P. Fanwick, Purdue University, USA

Keywords: $Na_5FeSi_4O_{12}$; crystal structure; Raman; glass; Mössbauer.

CCDC reference: 1872659

Supporting information: this article has supporting information at journals.iucr.org/c

The phase $Na_5FeSi_4O_{12}$ [pentasodium iron(III) silicate] crystallizes readily from the $Na_2O–Fe_2O_3–SiO_2$ glass system in a relatively large compositional range. However, its crystal structure and properties have not been studied in detail since its discovery in 1930. In this work, the $Na_5FeSi_4O_{12}$ phase was crystallized from a host glass with $5Na_2O{\cdot}Fe_2O_3{\cdot}8SiO_2$ stoichiometry, and both the glass and the crystal were studied. It was found that the $Na_5FeSi_4O_{12}$ phase crystallizes at ~720 °C from the glass and melts at ~830 °C when heated at a rate of 10 °C min^{-1}. The crystal structure was solved using single-crystal X-ray diffraction and the refined data are reported for the first time for the $Na_5FeSi_4O_{12}$ phase. It exhibits trigonal symmetry, space group $R\bar{3}c$, with a = 21.418 and c = 12.2911 Å. The Na atoms located between adjacent structural channels exhibit positional disorder and splitting which was only refined by using low-temperature data collection (150 K). While ~7% of the total Fe cations occur as Fe^{2+} in the glass, four-coordinated Fe^{3+} constitutes ~93% of the total Fe cations. However, iron in the crystal, which exhibits a paramagnetic behavior, is solely present as six-coordinated Fe^{3+}. The magnetic and vibrational properties of the glass and crystal are discussed to provide additional insight into the structure.

1. Introduction

The sodium iron silicate 5.1.8 phase ($5Na_2O{\cdot}Fe_2O_3{\cdot}8SiO_2$ or $Na_5FeSi_4O_{12}$) was first discovered by Bowen *et al.* (1930) in their study of the ternary phase diagram of $Na_2O–Fe_2O_3–SiO_2$. This phase is a binary compound of Na_2SiO_3 (sodium metasilicate) and $NaFeSi_2O_6$ (aegirine, also known as acmite), and melts congruently at 838 °C. Sodium metasilicate is a well-known compound of the chain sodium silicate family with an orthorhombic crystal system (McDonald & Cruickshank, 1967), while aegirine (monoclinic $C2/c$; Cameron *et al.*, 1973) is an end-member of the pyroxene group, which are important rock-forming minerals present in large abundances throughout Earth and other celestial bodies (Bowen *et al.*, 1930; Bailey & Schairer, 1966). These two phases are incompatible and can form the $Na_5FeSi_4O_{12}$ phase in systems where they co-exist. Bowen *et al.* (1930) also pointed out that $Na_5FeSi_4O_{12}$ is attacked slowly by cold water and strongly by boiling water. This could explain why $Na_5FeSi_4O_{12}$ has not yet been found in nature, despite its make-up from common elements. Although powder X-ray diffraction data of $Na_5FeSi_4O_{12}$ was previously published by Shannon *et al.* (1978), there have been few studies on this phase since then. To the best of our knowledge, there are no published structural data for Fe-based 5.1.8. However, the structure of $Na_5MSi_4O_{12}$-type silicates was first reported by Maximov *et al.* (1974), where M = Y, and later discussed by others (Shannon *et al.*, 1977, 1978; Beyeler &

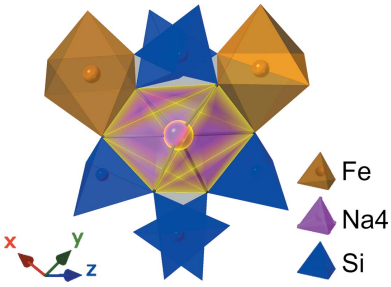

Table 1
Experimental details.

Crystal data	
Chemical formula	$Na_5FeSi_4O_{12}$
M_r	474.27
Crystal system, space group	Trigonal, $R\bar{3}c$
Temperature (K)	150
a, c (Å)	21.418 (3), 12.2911 (18)
V (Å^3)	4883.0 (16)
Z	18
Radiation type	Mo $K\alpha$
μ (mm^{-1})	2.10
Crystal size (mm)	0.02 × 0.01 × 0.003
Data collection	
Diffractometer	Bruker SMART APEXII three-circle
Absorption correction	Multi-scan (*SADABS*; Krause *et al.*, 2015)
T_{min}, T_{max}	0.640, 0.746
No. of measured, independent and observed [$I > 2\sigma(I)$] reflections	15291, 1108, 892
R_{int}	0.069
(sin $\theta/\lambda)_{max}$ (Å^{-1})	0.625
Refinement	
$R[F^2 > 2\sigma(F^2)]$, $wR(F^2)$, S	0.019, 0.046, 1.01
No. of reflections	1108
No. of parameters	118
$\Delta\rho_{max}$, $\Delta\rho_{min}$ (e Å^{-3})	0.37, −0.35

Computer programs: *APEX2* (Bruker, 2014), *SAINT* (Bruker, 2014), *SHELXT* (Sheldrick, 2015*a*), *SHELXL2013* (Sheldrick, 2015*b*) and *CrystalMaker* (*CrystalMaker*, 2018).

Hibma, 1978; Maximov *et al.*, 1982). The present work describes studies on the properties and structure of $5Na_2O{\cdot}Fe_2O_3{\cdot}8SiO_2$ glass, obtained from melt-quenching, and the $Na_5FeSi_4O_{12}$ phase, obtained by crystallization from the stoichiometric glass. The crystal structure, thermal analysis, Raman vibrational modes, Mössbauer spectroscopy and magnetic properties are presented.

2. Experimental

2.1. Synthesis and crystallization

The glass batch was prepared using Na_2CO_3 (Fisher Scientific, >99%), Fe_2O_3 (Alfa Aesar, 98%) and SiO_2 (US Silica, 99.7%) powders as starting materials. The mixed powders were melted in air at 1500 °C for 1 h in a platinum–10% rhodium crucible to make ∼20 g of the glass. The melt was poured onto an Inconel plate to quench and form a dark-green colored glass. The quenched glass was then crushed into powders, and ∼1 g was isothermally heat treated at 700 °C for 24 h to crystallize the $Na_5FeSi_4O_{12}$ phase (polycrystalline). The heat-treated sample was removed from the furnace and cooled in air.

2.2. Instrumental techniques

The as-quenched glass was crushed and sieved to obtain a particle size range of 63–125 µm for thermal analysis measurements. Differential scanning calorimetry (DSC) data were collected using an SDT Q600-TA Instruments system in the temperature range 30–1400 °C and a heating rate of 10 °C min^{-1} under a constant N_2 flow.

Powder X-ray diffraction (XRD) scans were obtained using an X'Pert Pro MPD (PANalytical, Netherlands) with Co $K\alpha$ radiation (λ = 0.1789 nm) at 40 kV and 40 mA. Data analysis was performed using *HighScore Plus* software (PANalytical, Netherlands).

A vibrating sample magnetometer (PMC3900, Lakeshore Cryotronics, Westerville, OH) with a maximum applied field of 1.8 T was employed to determine the magnetic hysteresis behavior of the $Na_5FeSi_4O_{12}$ phase. A field increment of 10 mT was used.

Room-temperature ^{57}Fe Mössbauer spectra were collected relative to α-Fe over a velocity range of ±12 mm s^{-1} using a constant acceleration spectrometer with a 25 mCi source of ^{57}Co in Rh. Attempts were made to fit the spectra using Lorentzian paramagnetic doublets consistent with Fe^{3+} and/or Fe^{2+}, using any *Recoil* analysis software package (Rancourt, 1998). However, at least three doublets were required in order to obtain robust fits for the glass sample using this fitting method. Therefore, instead, Extended Voigt-Based Fitting (xVBF) was used, as has also been used successfully to fit Mössbauer spectra for similar materials. The xVBF method provided robust fits with acceptable χ^2 using only two doublets to fit the glass spectrum – one each representing Fe^{2+} and Fe^{3+} – and using one singlet to fit the crystal spectrum. The determined iron redox ratio, $Fe^{3+}/\Sigma Fe$, is based on fitted peak areas and assumes that the recoil-free fraction ratio $f(Fe^{3+})/f(Fe^{2+}) = 1.0$.

In addition to Mössbauer spectroscopy, a solution-based spectrophotometric method (wet chemistry) was used to determine the iron redox state. In this method, 50 mg of the sample powder was dissolved in 1 ml hydrofluoric acid (48–51% HF, JT Baker) and 1 ml sulfuric acid (H_2SO_4, JT Baker). The solution was then diluted to 100 ml with distilled water, and 2 ml of the latter was added to 25 ml distilled water in a separate beaker. Using ammonium acetate buffer, its pH was adjusted to be in the range 3.5–4.5. 1,10-Phenanthroline (5 ml) solution (*i.e.* 100 mg 1,10-phenanthroline dissolved in 100 ml distilled water) was added to react with Fe^{2+} and add a pink color to the solution according to Fe^{2+} concentration. The colored solution was diluted and transferred to a 1 cm plastic cuvette to measure the absorbance at 520 nm using a UV–Vis spectrometer (Thermo Scientific Evolution 260 Bio). Using an Fe^{2+} standard curve obtained from standard solutions with known concentrations of Fe^{2+}, the concentration of Fe^{2+} in the unknown solution was calculated. To measure the total Fe concentration in the unknown solution, a small scoop of hydroxylamine (reductant) was added to the remainder of the solution, which was then warmed below boiling temperature to reduce all Fe to Fe^{2+}, and the absorbance of the reduced solution corresponded to the total Fe. More details of the procedure can be found in Weaver *et al.* (2015, and references therein).

Raman spectroscopy analysis was performed on solid unpolished pieces using a diode-pumped solid-state laser (Ventus, Laser Quantum, UK) at 532 nm with a laser output at

Table 2
Bond valence sums (valence units*) for $Na_5FeSi_4O_{12}$.

BVS for disordered Na atoms (Na51, Na52 and Na53) are not included. These disordered Na atoms contribute limited BV to atoms O2, O3, O4, O5 and O6, depending on site occupancy.

Atoms	Fe1	Si1	Si2	Na1	Na2	Na3	Na4	Na5	Sum
O1			1.10	0.20 ×6↓	0.16 ×6↓	0.22/0.20/0.05			1.92
O2	0.52 ×2↓	1.07				0.04	0.19 ×2↓	0.08 ×2↓	2.06
O3	0.47 ×2↓		1.04			0.23		0.14 ×2↓	1.87
O4		0.90	0.91			0.04	0.14 ×2↓		1.96
O5		0.94	0.90			0.22			2.06
O6	0.51 ×2↓	1.10					0.18 ×2↓	0.28 ×2↓	2.07
Sum	3.00	4.01	3.95	1.18	0.95	0.99	1.03	1.01	

Note: (*) bond valence parameters are from Gagné & Hawthorne (2015).

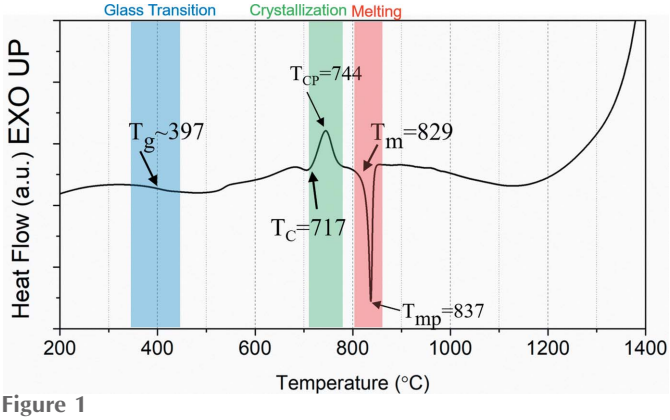

Figure 1
DSC heating scan of 5.1.8 ($5Na_2O{\cdot}Fe_2O_3{\cdot}8SiO_2$) glass obtained at 10 °C min^{-1} in an N_2 flow.

the sample of 50 mW. Detection was performed with a liquid-nitrogen-cooled SPEX 500M single monochromator and a 200 µm slit using backscattering geometry with an InPhotonics RPB Laboratory Probe. Reported spectra were averaged over ten pulse collections for 10 s each.

2.3. Structure determination and refinement

Crystal data, data collection and structure refinement details are summarized in Table 1. The heat-treated sample was crushed and the particles were examined using a polarized light microscope. Crystals of $Na_5FeSi_4O_{12}$ range from ~1 µm up to 20 µm wide. A red–orange thin plate (20 × 10 × 3 µm) exhibiting a sharp extinction under cross-polarized light was selected and mounted on a MiTeGen CryoLoop for the single-crystal X-ray diffraction experiment. All atoms except for the disordered Na atoms were refined successfully with anisotropic displacement parameters. The occupancies of atoms Na5, Na51, Na52 and Na53 were allowed to refine freely to obtain site-occupancy factors based on the diffraction data. The sum of the refined site occupancies (0.987) confirms the expected stoichiometry for the structure and an overall formula with 4.96 (ideally 5) Na atoms per formula unit. Table 2 lists bond valence sums for $Na_5FeSi_4O_{12}$ and Table 3 lists selected interatomic distances.

3. Results and discussion

3.1. Thermal analysis

Fig. 1 shows the DSC heating scans of the $5Na_2O{\cdot}Fe_2O_3{\cdot}8SiO_2$ as-quenched glass. The critical temperatures corresponding to glass transition (T_g), onset of crystallization (T_C), peak of crystallization (T_{CP}), onset of melting (T_m) and peak of melting (T_{mp}) are marked on the curve. The DSC scan

Table 3
Selected interatomic distances (Å) for $Na_5FeSi_4O_{12}$.

Refined occupancies: Na5 0.682 (7), Na51 0.144 (9), Na51 0.145 (10) and Na53 0.017 (7).

Fe1—O2	2.038 (2)	Na1—O1	2.377 (2)	Na4—O2	2.386 (2)	Na52—O2	2.396 (8)
Fe1—O3	2.034 (2)			Na4—O4	2.516 (2)	Na52—O3	2.411 (9)
Fe1–O6	2.002 (2)	Na2—O4	2.467 (2)	Na4—O6	2.413 (2)	Na52—O4	2.640 (11)
<Fe1—O>	2.025			*<Na4—O>*	2.438	Na52—O4	2.862 (12)
						Na52—O5	2.445 (10)
Si1—O2	1.597 (2)	Na3—O1	2.330 (2)	Na5—O2	2.738 (2)	Na52—O6	2.546 (15)
Si1—O4	1.663 (2)	Na3—O1	2.378 (2)	Na5—O3	2.533 (2)	*<Na52—O>*	2.550
Si1—O5	1.650 (1)	Na3—O1	2.946 (2)	Na5—O6	2.422 (1)		
Si1—O6	1.587 (2)	Na3—O2	3.097 (2)	*<Na5—O>*	2.564	Na53—O2	2.86 (11)
<Si1—O>	1.624	Na3—O3	2.320 (2)			Na53–O3	2.53 (12)
		Na3—O4	3.020 (2)	Na51—O2	2.295 (8)	Na53—O4	2.63 (12)
Si2—O1	1.587 (2)	Na3—O5	2.331 (2)	Na51–O3	2.359 (10)	Na53—O4	2.66 (12)
Si2—O3	1.610 (2)	*<Na3—O>*	2.632	Na51—O4	2.899 (12)	Na53—O5	2.33 (13)
Si2—O4	1.661 (1)			Na51—O5	2.552 (11)	Na53—O5	2.96 (13)
Si2—O5	1.664 (2)			Na51—O6	2.414 (6)	Na53—O6	2.57 (10)
<Si2—O>	1.631			*<Na51—O>*	2.504	*<Na53—O>*	2.65

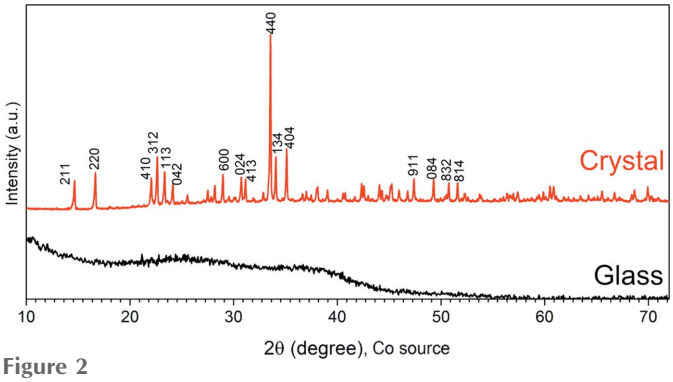

Figure 2
XRD patterns of 5.1.8 ($5Na_2O{\cdot}Fe_2O_3{\cdot}8SiO_2$) as-quenched glass and the crystallized powder heat-treated at 700 °C for 24 h. The numbers in the crystal pattern refer to the most intense lattice planes (*hkl*) from the reference powder pattern.

shows a subtle glass transition temperature of $T_g \sim 397$ °C for the 5.1.8 glass. The crystallization of $Na_5FeSi_4O_{12}$ takes place in the range 700–780 °C, identified from a relatively sharp exothermic peak (T_C = 717 and T_{CP} = 744 °C). The intense sharp endothermic peak close to crystallization corresponds to the melting of $Na_5FeSi_4O_{12}$ crystals, with T_m = 829 °C and T_{mp} = 837 °C. The melting peak temperature (T_{mp}) obtained from our DSC scan is close to the congruent melting point of this phase reported by Bowen *et al.* (1930) (*i.e.* 838 °C).

3.2. Phase analysis

The powder XRD pattern of the as-quenched glass is presented in Fig. 2 which confirms the amorphous state of the glass. The glass powder was then heat treated at 700 °C for 24 h to crystallize the $Na_5FeSi_4O_{12}$ phase. The powder XRD pattern of the crystallized $Na_5FeSi_4O_{12}$ shown in Fig. 2 indicates that the glass transforms into $Na_5FeSi_4O_{12}$ crystals upon heat treatment. This pattern is consistent with the powder XRD data of the $Na_5FeSi_4O_{12}$ phase published by Shannon *et al.* (1978) (PDF# 032-1102).

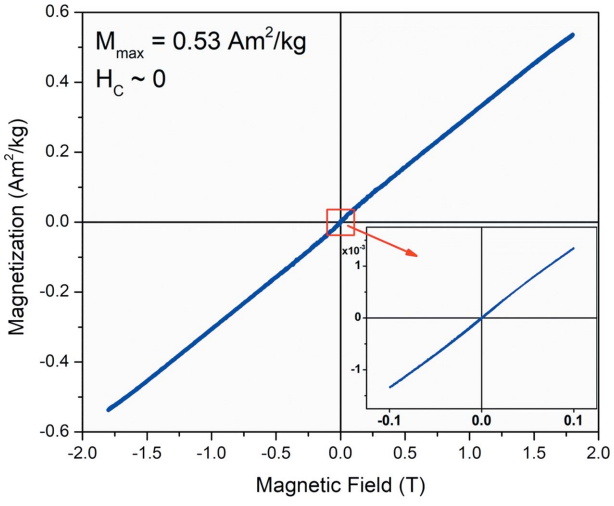

Figure 3
Magnetization–magnetic field curve of the crystallized $Na_5FeSi_4O_{12}$ phase.

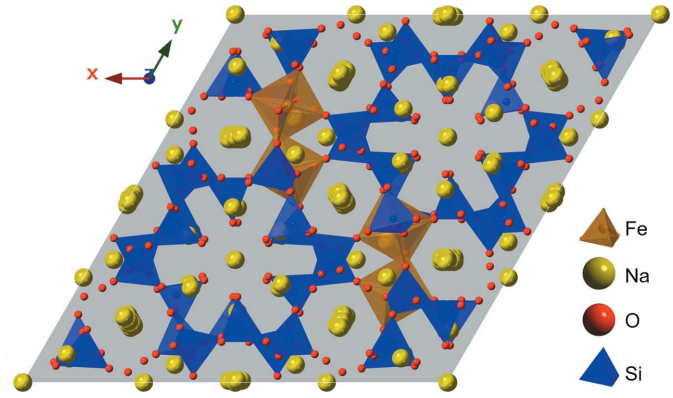

Figure 4
A representation of the entire unit cell of the $Na_5FeSi_4O_{12}$ structure, viewed along the *c* axis. Fe occupies a single unique crystallographic site, while there are two unique tetrahedral Si atoms. The 12-membered $Si_{12}O_{36}$ rings are formed by alternating Si1 tetrahedra (pointing outwards) and Si2 tetrahedra (pointing inwards). Na occurs in eight independent sites, several with a disordered nature.

3.3. Magnetic analysis

Room-temperature magnetization *versus* magnetic field of the crystallized $Na_5FeSi_4O_{12}$ phase is presented in Fig. 3. The loop, however, does not show any hysteresis behaviour ($H_C \sim 0$). Moreover, it reveals a linear dependency and no trend toward magnetic saturation, with a maximum magnetization of 0.53 Am^2/kg at H_{max} = 1.8 T. Such a behaviour asserts the paramagnetic nature of the $Na_5FeSi_4O_{12}$ iron-containing magnetic phase.

3.4. Crystal structure

The crystal structure of $Na_5FeSi_4O_{12}$ is built from a heteropolyhedral framework of Fe–O, Si–O and Na–O polyhedra (Fig. 4). There is one crystallographically unique Fe atom, with an average Fe—O bond length of 2.025 Å. Each Fe—O bond is made to O atoms from surrounding silicate groups by sharing vertices. There are two unique tetrahedral Si atoms, with an average Si—O bond length of 1.627 Å, which form rings of 12 vertex-sharing tetrahedra ($Si_{12}O_{36}$), with alternating Si1 and Si2 atoms stacked along the *c* axis. Adja-

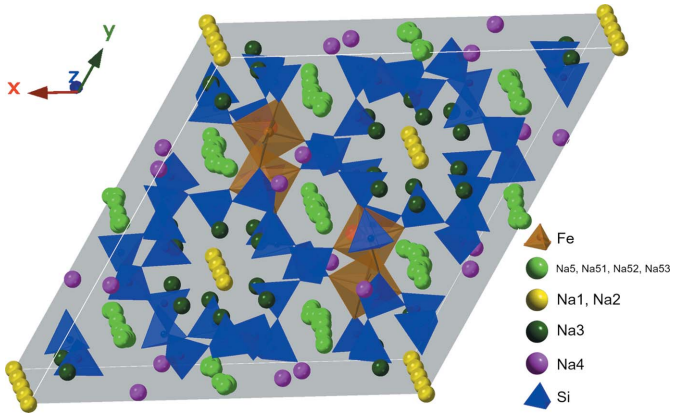

Figure 5
A mixed polyhedral and ball-and-stick representation of the unit cell of $Na_5FeSi_4O_{12}$. Unique Na atoms are depicted with contrasting colours.

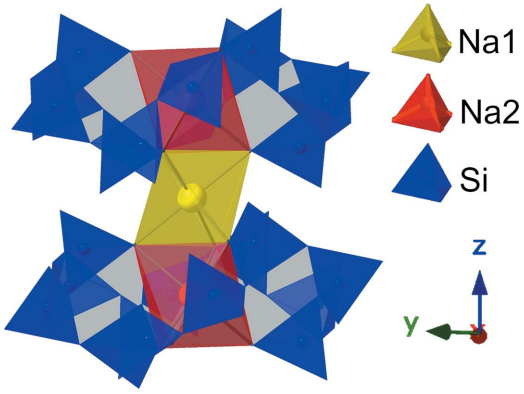

Figure 6
Na1 and Na2 octahedra within the channels of the 12-membered rings of Si tetrahedra, viewed along the *b* axis.

cent $Si_{12}O_{36}$ rings are linked by Fe^{3+} octahedra. Eight independent Na positions occur in the $Na_5FeSi_4O_{12}$ structure and display a variety of coordination environments (Fig. 5). Atoms Na1 and Na2, stacked within the 12-membered rings ($Si_{12}O_{36}$), are six-coordinate plane-sharing octahedra with only slight distortions (Fig. 6), whereas the Na3 atom forms a highly irregular coordination environment with six O atoms of surrounding silicate groups. As illustrated in Fig. 7, atom Na4 exhibits a strongly distorted octahedral arrangement, with equatorial bonds adopting an interesting tetragonal distortion. Several disordered Na atoms, *i.e.* Na5, Na51, Na52 and Na53, with refined occupancies of 0.682 (7), 0.144 (9), 0.145 (10) and 0.017 (7), respectively, reside irregularly along the *c* axis in the spaces between adjacent 12-membered rings channels. Na5 takes the shape of a trigonal antiprism and bonds to six O atoms of silicate groups of the ring. The remaining disordered Na atoms (Na51, Na52 and Na53) are irregularly shaped and bond with five or six O atoms of ring silicate groups. From the refinement, the formula for the crystal studied here is $Na_{4.96}FeSi_4O_{12}$.

The structure of $Na_5FeSi_4O_{12}$ is isotypic with sodium rare-earth silicates (Sc and Y) of the same stoichiometry (Maximov *et al.*, 1982), except for the arrangement of the disordered Na atoms. In the crystal structures of $Na_5YSi_4O_{12}$ and $Na_5ScSi_4O_{12}$ at room temperature (and also at 300 °C for the

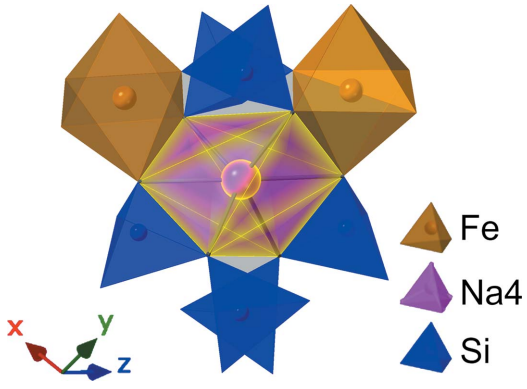

Figure 7
The tetrahedrally distorted Na4 octahedron.

Table 4
Comparison of the unit-cell parameters of $Na_5FeSi_4O_{12}$ to analogues from Shannon *et al.* (1978) (unless otherwise noted).

Phase	*a* (Å)	*c* (Å)	*V* (Å)
$Na_5FeSi_4O_{12}$ (this study)	21.418 (3)	12.291 (18)	4883
$Na_5FeSi_4O_{12}$	21.425 (2)	12.300 (2)	4889
$Na_5ScSi_4O_{12}$	21.672 (3)	12.437 (2)	5058
$Na_5ScSi_4O_{12}$ (Maximov *et al.*, 1982)	21.679 (6)	12.446 (3)	5066
$Na_5InSi_4O_{12}$	21.725 (2)	12.460 (2)	5093
$Na_5LuSi_4O_{12}$	21.920 (2)	12.576 (2)	5233
$Na_5YbSi_4O_{12}$	21.940 (2)	12.567 (2)	5239
$Na_5TmSi_4O_{12}$	21.958 (3)	12.579 (2)	5252
$Na_5ErSi_4O_{12}$	21.989 (2)	12.610 (2)	5280
$Na_5HoSi_4O_{12}$	22.034 (2)	12.607 (2)	5301
$Na_5YSi_4O_{12}$	22.035 (1)	12.604 (1)	5300
$Na_5YSi_4O_{12}$ (Maximov *et al.*, 1982)	22.062 (8)	12.621 (4)	5320
$Na_5DySi_4O_{12}$	22.058 (2)	12.623 (3)	5319
$Na_5TbSi_4O_{12}$	22.083 (1)	12.627 (1)	5332
$Na_5GdSi_4O_{12}$	22.126 (5)	12.650 (4)	5363
$Na_5SmSi_4O_{12}$	22.164 (4)	12.661 (4)	5386

Y analogue), only two Na sites are refined with highly prolate displacement parameters along *c*, which should have been treated as split positions. Distinct Na locations from the splitting disorder became more apparent in $Na_5FeSi_4O_{12}$ by using low-temperature data collection, but splitting differences observed here could also arise from the smaller ionic radius of $^{[6]}Fe^{3+}$ (high spin; 0.645 Å) relative to $^{[6]}Y^{3+}$ (0.900 Å), or $^{[6]}Sc^{3+}$ (0.745 Å) (Shannon, 1976). The cation size difference is also manifested in the measured unit-cell parameters for each phase (Table 4). Furthermore, the disordered nature of the Na atoms along the *c* axis in $Na_5MSi_4O_{12}$ (*M* = Fe, Y, Sc, In, Lu and Sm) phases is direct evidence of their relatively high ionic conductivity. Based on measurements by Shannon *et al.* (1978), $Na_5FeSi_4O_{12}$ exhibited the lowest conductivity of all related phases. Their measurements reveal a linear dependence of the trivalent cation radius to conductivity, whereby smaller cations lead to lower conductivity. The effect is presumably due to excess empty channel space (Maximov *et al.*, 1982), since the size of the channel is not strongly affected by the identity of the trivalent cation. The O···O distances between channels in the silicate ring range from 4.81 to 4.99 Å in the Fe analogue and from 4.85 to 5.02 Å in the Y analogue, as measured from equivalent proximal O-atom pairs (O1 in $Na_5FeSi_4O_{12}$ and O3 in $Na_5YSi_4O_{12}$; Maximov *et al.*, 1974).

3.5. Spectroscopic analyses

Room-temperature ^{57}Fe Mössbauer spectra of the 5.1.8 glass and $Na_5FeSi_4O_{12}$ were obtained and fitted by two xVBF doublets and one xVBF singlet, respectively (Fig. 8). Fitting parameters and relative areas are presented in Table 5. The 5.1.8 glass Mössbauer spectrum (Fig. 8*a*) shows two overlapping doublets typical of iron-bearing silicate glasses. The doublet with lower chemical shift (CS) and quadrupole splitting (QS) represents ferric iron (Fe^{3+}), while the doublet with higher CS and QS is assigned to ferrous iron (Fe^{2+}), both of which are present in the amorphous phase (Mysen & Richet, 2005; Dyar *et al.*, 2006). The spectrum and fitted parameters

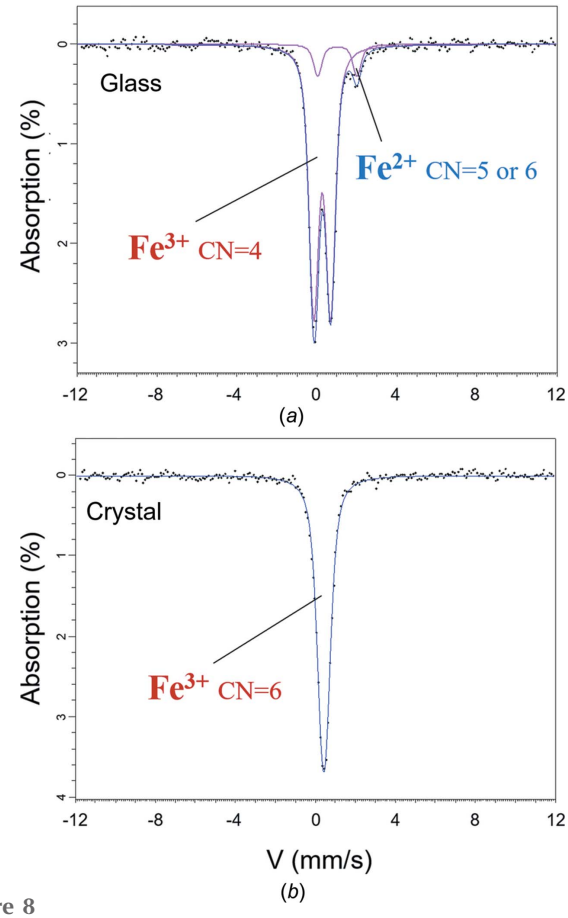

Figure 8
Fitted Mössbauer spectra of 5.1.8 ($5Na_2O{\cdot}Fe_2O_3{\cdot}8SiO_2$) for (*a*) the as-quenched glass and (*b*) the crystallized powder heat treated at 700 °C for 24 h.

indicate that the large majority of Fe in the glass is present as Fe^{3+}. Based on the obtained values of CS and QS, and those reported in the literature (*e.g.* Dyar, 1985; Dyar *et al.*, 2006; Mysen & Richet, 2005), the Fe^{3+} ions are predominantly fourfold coordinated, whereas the Fe^{2+} ions exhibit higher coordination (five- or sixfold). This result is consistent with the common observation that, in Fe-bearing silicate glasses, Fe^{3+} is primarily tetrahedrally coordinated and acts as a network-forming cation (similar to Al^{3+}), while Fe^{2+} cations are found to play the role of a network modifier (similar to Mg^{2+}) with higher coordination numbers ranging from 4 to 6 (Mysen, Seifert *et al.*, 1980; Bingham *et al.*, 1999; Kim *et al.*, 2016). Fig. 8(*b*) presents the Mössbauer spectrum of the crystalline sample after the glass is crystallized to form the $Na_5FeSi_4O_{12}$ crystalline phase. Unlike the glass, the crystal shows one singlet, indicative of a single iron species in a symmetrical site in the crystallized sample. Singlet (or doublet) features, instead of sextet(s), confirm the paramagnetic behaviour of the crystal that was previously revealed by magnetic measurements (Fig. 3). Komatsu & Soga (1980) have also shown that the doublet changes to a singlet (or a very narrow doublet) in the crystallization process of 5.1.8 glass. The CS value of the singlet in our spectrum (0.42 mm s^{-1}), which is close to what Komatsu & Soga (1980) and Mysen, Seifert *et al.*

Table 5
xVBF fitting parameters for the Mössbauer spectra of the 5.1.8 glass and crystal.

Sample	Signal	CS[1] ±0.02 (mm s^{-1})	QS[2] ±0.02 (mm s^{-1})	Area ±2 (%)	Fit reduced χ^2
Glass	Doublet 1 (Fe^{3+})	0.26	0.85	90.1	0.614
	Doublet 2 (Fe^{2+})	1.02	1.97	9.9	
Crystal	Singlet 1 (Fe^{3+})	0.42		100	0.852

Notes: (1) chemical shift relative to α-Fe foil; (2) quadrupole splitting.

Table 6
Iron redox values determined from Mössbauer spectroscopy and wet chemistry for the 5.1.8 glass and crystal.

			Glass	Crystal
$Fe^{3+}/\Sigma Fe$	Mössbauer Spectroscopy		0.901	1.000
	Wet chemistry (triplicates)	Average	0.927	0.994
		Standard Deviation	0.017	0.001

(1980) reported (0.38 mm s^{-1}) for this phase, is consistent with six-coordinated Fe^{3+} in the crystal. Moreover, the very small or zero QS value (singlet) of the Fe^{3+} ions in the crystal, unlike the glass, indicates that the site distortion of the Fe^{3+} ions in the quenched glass is removed upon crystallization. In other words, the Fe^{3+} ion sites are non-identical and distorted in the glass phase in comparison with those in the crystals (Komatsu & Soga, 1980; Hirao *et al.*, 1980).

Table 6 lists the iron redox values ($Fe^{3+}/\Sigma Fe$) of the 5.1.8 glass and crystal samples obtained from Mössbauer spectra and the wet chemistry method. $Fe^{3+}/\Sigma Fe$ values from Mössbauer were determined by the ratio of the Fe^{3+} doublet area to the total spectral area. Both methods reveal consistent values for the Fe redox state. While the 5.1.8 glass appears to contain ∼10% ferrous iron fraction, the Fe ions in the crystalline sample are fully oxidized to Fe^{3+} [according to Mössbauer fitted areas and assuming $f(Fe^{3+})/f(Fe^{2+}) = 1.0$]. The value of $f(Fe^{3+})/f(Fe^{2+})$ is dependent on the host matrix and, for some oxide minerals and glasses, can deviate from the value of 1.0. When this occurs in oxide glasses it usually results in a slight overestimation of the Fe^{3+} content, based on fitted Fe^{3+} and Fe^{2+} areas (Zhang *et al.*, 2018). The recoil-free fractions of Fe^{2+} and Fe^{3+} in the glass studied here are unknown, but evidence for multiple oxide minerals and glasses, summarized recently by Zhang *et al.* (2018), suggests a slight overestimation of the Fe^{3+} content. However, redox quantification is further complicated by the presence of asymmetry in the Fe^{2+} doublet. In fitting Mössbauer spectra for highly reduced glasses, in which the majority of iron is present as Fe^{2+}, taking account of this asymmetry is important (Jayasuriya *et al.*, 2004). However, in spectra for oxidized glasses, in which the low-velocity part of the weak Fe^{2+} doublet overlaps with the low-velocity part of the strong Fe^{3+} doublet, the Fe^{2+} doublet asymmetry has not been fitted (Jayasuriya *et al.*, 2004), presumably because its effect on the fitted parameters and areas is considered acceptably small or negligible. Consequently, it has not been attempted here. Overall, we can conclude that the Mössbauer-determined iron redox ratio for our glass sample is consistent

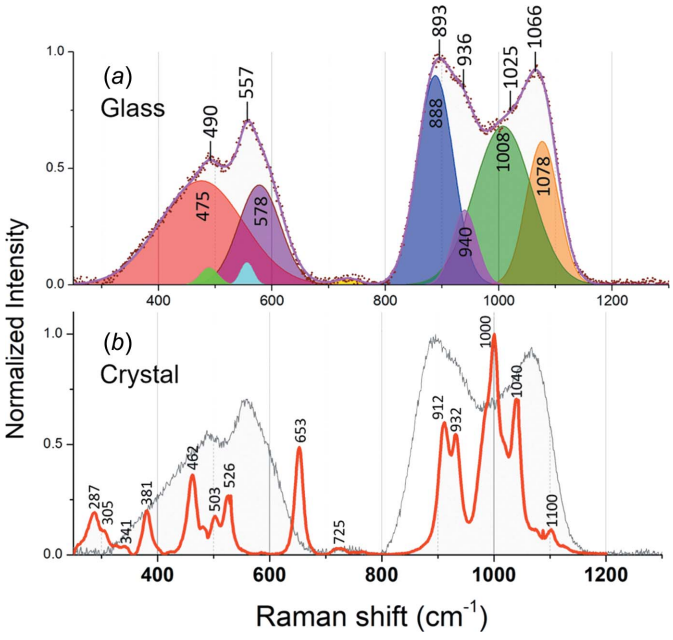

Figure 9
Normalized Raman spectra of 5.1.8 ($5Na_2O{\cdot}Fe_2O_3{\cdot}8SiO_2$) for (*a*) the as-quenched glass with Gaussian deconvolution peak fitting and (*b*) the crystallized sample heat treated at 700 °C for 24 h (in red).

with the value determined by the (more accurate) wet chemical analysis, within the uncertainties due to fitting and any differences in the Fe^{2+} and Fe^{3+} recoil-free fraction ratios.

Fig. 9(*a*) shows the Raman spectrum of the $5Na_2O{\cdot}Fe_2O_3{\cdot}8SiO_2$ as-quenched glass, deconvoluted into Gaussian bands. The Raman spectra of most silicate glasses show three regions which correspond to different types of vibration: low frequency (LF ~200–600 cm^{-1}), medium frequency (MF ~600–800 cm^{-1}) and high frequency (HF ~800–1200 cm^{-1}). LF and HF bands are the most intense features in silicate glasses, as revealed by the Raman spectrum of 5.1.8 glass (Fig. 9*a*). The bands of the LF region in silicate networks are conventionally assigned to vibrations of the bridging oxygens (*i.e.* $^0O-T-O^0$ linkage, where T = Si and Fe^{3+}) in various Q^n species. These vibrations can potentially reveal some information about the inter-tetrahedral angle and the ring arrangement. The LF envelope can be deconvoluted into bands presenting $Si-O^0$ rocking motions in fully polymerized (Q^4) three-dimensional network species and Si—O—Si bending motions in glasses with nonbridging oxygens (NBOs) (Neuville *et al.*, 2014; Di Muro *et al.*, 2009; Mysen, Virgo *et al.*, 1980; Di Genova *et al.*, 2016). Moreover, the bands related to vibrations of oxygen bonds linked to alkali and alkali earth metals, and to six (or higher) coordinated transition metals appear in this region (Rossano & Mysen, 2012). The 5.1.8 glass Raman spectrum shows a minimum of two resolved peaks in the LF band. The relatively intense LF envelope can be taken as diagnostic of $T-O-T$ linkages, *i.e.* bridging oxygens, within the glass structure. Note that two low-intensity peaks, in addition to the two main peaks, were used to fit the LF band, as it is not possible to fit the LF envelope with only two Gaussian peaks. The main low-frequency bands are near 490 and 557 cm^{-1}. The feature at ~490 cm^{-1} is attributed to the symmetric stretching of bridging oxygens (BOs), *i.e.* $\nu_s(T-O-T)$ (Wang *et al.*, 1993). The stronger band near 557 cm^{-1} is assigned to the vibration of BOs from Q^3 units, since it has been observed by Wang *et al.* (1993) that its intensity increases by increasing the NBO/T (*i.e.* nonbridging oxygens per tetrahedron) from 0 to 0.5 in the Na_2O–Fe_2O_3–SiO_2 system. Assuming that all the Fe is present in tetrahedral coordination, NBO/T = 1 in the 5.1.8 glass structure, which results in an increased intensity of the 557 cm^{-1} band. However, as discussed in the Mössbauer spectroscopy section, a smaller portion of the Fe ions exists as higher-coordinated Fe^{2+} within the glass structure, which leads to more NBOs and thus NBO/T is between 1 and 2. It is suggested that for this range of average ratio of NBOs to tetrahedrally coordinated T cations, the glass structure is dominated by Q^1, Q^2 and Q^3 species (Wang *et al.*, 1993). The HF envelope normally relates to NBO-bearing units since it is attributed to symmetric $T-O$ stretching vibrations in different Q^n units, where n = 0, 1, 2 and 3. It is very weak in silica glass (mostly Q^4) and gets more intense in silicates with nonbridging oxygens (Neuville *et al.*, 2014; Rossano & Mysen, 2012; McMillan, 1984). Therefore, the multiple peaks appearing in the HF envelope of 5.1.8 glass is a result of variations in its Q^n species. 5.1.8 glass shows two HF well-resolved peaks (~893 and 1066 cm^{-1}). However, the asymmetry of these peaks indicates that each of them, in fact, consists of at least two unresolved peaks, *i.e.* a shoulder near ~936 cm^{-1} and a band near 1025 cm^{-1}. In the HF region of the Raman spectra of alkali and alkali earth silicate glasses, the band attributed to stretching vibrations of the Q^n species has a greater frequency than that of $Q^{n'}$, if $n > n'$, while n and n' are 0, 1, 2 or 3 (*e.g.* McMillan, 1984; Mysen, Virgo *et al.*, 1980; Baert *et al.*, 2011; Neuville, 2006). In other words, the bands at ~850, ~900, 950–1000 and 1050–1100 cm^{-1} are generally assigned to vibrations of silicate tetrahedra with four, three, two and one NBO, respectively. The peak near ~940 cm^{-1}, however, is observed to be still intense even for highly polymerized three-dimensional networks in Na—Fe—Si systems (Wang *et al.*, 1993; Mysen, Seifert *et al.*, 1980), and is assigned to the antisymmetric vibrations of BOs [$\nu_{as}(T-O-T)$] in such glasses. The lower-frequency band (~890 cm^{-1}) is due to NBOs and likely $^-O-(Fe,Si)-O^-$ stretching vibrations (Mysen, Seifert *et al.*, 1980), where O^- indicates bridging oxygens. The bands at higher frequency (~1050 cm^{-1}), whose intensities increase considerably by depolymerization of Na—Fe—Si glasses (Wang *et al.*, 1993; Mysen, Seifert *et al.*, 1980), are assigned to $^-O-(Fe,Si)-O^0$ stretching mostly in Q^3 units, where O^0 indicates bridging oxygens. Therefore, the Q^2 (chain) and Q^3 (sheet) species are dominant in the 5.1.8 glass structure, as reported by Mysen, Seifert *et al.* (1980) for similar compositions.

Fig. 9(*b*) shows the Raman spectrum of crystalline $Na_5FeSi_4O_{12}$ (red) compared to the spectrum of the corresponding glass (gray). This Raman spectrum is, to our knowledge, the first reported for this compound. The bands of the crystal spectrum are much sharper and their intensities are about an order of magnitude greater than those of the glass spectrum,

which is due to the long-range order of the crystal. The crystal spectrum is characterized by the most intense bands (four or five asymmetric bands) occurring in the 900–1100 cm^{-1} region, a relatively intense band at ~650 cm^{-1} and a few lower-intensity bands at frequencies below 550 cm^{-1}. Similar to silicate glasses, the bands in the 900–1100 cm^{-1} region of the silicate crystals are assigned to Si—O^- stretching vibrations (McMillan, 1984; Huang *et al.*, 2000). The symmetrical band at ~650 cm^{-1} is due to either Si—O^0 stretching modes or O—Si—O bending modes (Huang *et al.*, 2000; Buzatu & Buzgar, 2010). The low-frequency bands (<550 cm^{-1}) are attributed to Fe—O and Na—O bond vibrations in their polyhedra (Richet *et al.*, 1996; Katerinopoulou *et al.*, 2008; Buzatu & Buzgar, 2010).

Acknowledgements

The authors would like to acknowledge use of the Bruker SMART APEXII single-crystal diffractometer provided by the Nuclear Science Center at Washington State University. We would like to thank Emily Nienhuis and Jason Lonergan for their help in performing the Raman spectroscopy measurements.

Funding information

Funding for this research was provided by: The US Department of Energy's Waste Treatment & Immobilization Plant Project of the Office of River Protection managed by Albert A. Kruger.

References

Baert, K., Meulebroeck, W., Wouters, H., Cosyns, P., Nys, K., Thienpont, H. & Terryn, H. (2011). *J. Raman Spectrosc.* **42**, 1789–1795.
Bailey, D. K. & Schairer, J. F. (1966). *J. Petrol.* **7**, 114–170.
Beyeler, H. U. & Hibma, T. (1978). *Solid State Commun.* **27**, 641–643.
Bingham, P. A., Parker, J. M., Searle, T., Williams, J. M. & Fyles, K. (1999). *J. Non-Cryst. Solids*, **253**, 203–209.
Bowen, N. L., Schairer, J. F. & Willems, H. W. V. (1930). *Am. J. Sci. Ser. 5*, **20**, 405–455.
Bruker (2014). *APEX2*. Bruker AXS Inc., Madison, Wisconsin, USA.
Buzatu, A. & Buzgar, N. (2010). *An. Stiint. Univ. Al. I. Cuza Iasi. Sect. 2 Geol.* **56**, 107.
Cameron, M., Sueno, S., Prewitt, C. & Papike, J. (1973). *Am. Mineral.* **58**, 594–618.
CrystalMaker (2018). *CrystalMaker*. CrystalMaker Software, Bicester, Oxfordshire, England.
Di Genova, D., Hess, K. U., Chevrel, M. O. & Dingwell, D. B. (2016). *Am. Mineral.* **101**, 943–952.
Di Muro, A., Métrich, N., Mercier, M., Giordano, D., Massare, D. & Montagnac, G. (2009). *Chem. Geol.* **259**, 78–88.
Dyar, M. D. (1985). *Am. Mineral.* **70**, 304–316.
Dyar, M. D., Agresti, D. G., Schaefer, M. W., Grant, C. A. & Sklute, E. C. (2006). *Annu. Rev. Earth Planet. Sci.* **34**, 83–125.
Gagné, O. C. & Hawthorne, F. C. (2015). *Acta Cryst.* B**71**, 562–578.
Hirao, K., Komatsu, T. & Soga, N. (1980). *J. Non-Cryst. Solids*, **40**, 315–323.
Huang, E., Chen, C., Huang, T., Lin, E. & Xu, J. (2000). *Am. Mineral.* **85**, 473–479.
Jayasuriya, K. D., O'Neill, H. S. C., Berry, A. J. & Campbell, S. J. (2004). *Am. Mineral.* **89**, 1597–1609.
Katerinopoulou, A., Musso, M. & Amthauer, G. (2008). *Vib. Spectrosc.* **48**, 163–167.
Kim, H.-I., Sur, J. C. & Lee, S. K. (2016). *Geochim. Cosmochim. Acta*, **173**, 160–180.
Komatsu, T. & Soga, N. (1980). *J. Chem. Phys.* **72**, 1781–1785.
Krause, L., Herbst-Irmer, R., Sheldrick, G. M. & Stalke, D. (2015). *J. Appl. Cryst.* **48**, 3–10.
Maximov, B., Kharitonov, Y. A. & Belov, N. (1974). *Sov. Phys. Dokl.* p. 763.
Maximov, B. A., Petrov, I. V., Rabenau, A. & Schulz, H. (1982). *Solid State Ionics*, **6**, 195–200.
McDonald, W. S. & Cruickshank, D. W. J. (1967). *Acta Cryst.* **22**, 37–43.
McMillan, P. (1984). *Am. Mineral.* **69**, 622–644.
Mysen, B. O. & Richet, P. (2005). In *Silicate glasses and melts: properties and structure*. Amsterdam: Elsevier.
Mysen, B. O., Seifert, F. & Virgo, D. (1980). *Am. Mineral.* **65**, 867–884.
Mysen, B. O., Virgo, D. & Scarfe, C. M. (1980). *Am. Mineral.* **65**, 690–710.
Neuville, D. R. (2006). *Chem. Geol.* **229**, 28–41.
Neuville, D. R., de Ligny, D. & Henderson, G. S. (2014). *Rev. Mineral. Geochem.* **78**, 509–541.
Rancourt, D. (1998). *Recoil Mössbauer Spectral Analysis Software*. Ottawa: Intelligent Scientific Applications Inc.
Richet, P., Mysen, B. O. & Andrault, D. (1996). *Phys. Chem. Miner.* **23**, 157–172.
Rossano, S. & Mysen, B. (2012). In *EMU Notes in Mineralogy*, Vol. 12. http://eurominunion.org/.
Shannon, R. D. (1976). *Acta Cryst.* A**32**, 751–767.
Shannon, R. D., Chen, H. Y. & Berzins, T. (1977). *Mater. Res. Bull.* **12**, 969–973.
Shannon, R. D., Taylor, B. E., Gier, T. E., Chen, H. Y. & Berzins, T. (1978). *Inorg. Chem.* **17**, 958–964.
Sheldrick, G. M. (2015*a*). *Acta Cryst.* A**71**, 3–8.
Sheldrick, G. M. (2015*b*). *Acta Cryst.* C**71**, 3–8.
Wang, Z., Cooney, T. F. & Sharma, S. K. (1993). *Contrib. Mineral. Petrol.* **115**, 112–122.
Weaver, J. L., Wall, N. A. & McCloy, J. S. (2015). *MRS Proc.* **1744**, 93–100.
Zhang, H. L., Cottrell, E., Solheid, P. A., Kelley, K. A. & Hirschmann, M. M. (2018). *Chem. Geol.* **479**, 166–175.

supporting information

Acta Cryst. (2018). C**74** [https://doi.org/10.1107/S2053229618014353]

Structure and properties of $Na_5FeSi_4O_{12}$ crystallized from $5Na_2O$–Fe_2O_3–$8SiO_2$ glass

Mostafa Ahmadzadeh, Travis A. Olds, Alex Scrimshire, Paul A. Bingham and John S. McCloy

Computing details

Data collection: *APEX2* (Bruker, 2014); cell refinement: *APEX2* (Bruker, 2014); data reduction: *APEX2* (Bruker, 2014) and *SAINT* (Bruker, 2014); program(s) used to solve structure: SHELXT (Sheldrick, 2015a); program(s) used to refine structure: *SHELXL2013* (Sheldrick, 2015b); molecular graphics: *CrystalMaker* (*CrystalMaker*, 2018); software used to prepare material for publication: *SHELXL2013* (Sheldrick, 2015a).

Pentasodium iron(III) silicate

Crystal data

$Na_5FeSi_4O_{12}$
M_r = 474.27
Trigonal, $R\bar{3}c$
a = 21.418 (3) Å
c = 12.2911 (18) Å
V = 4883.0 (16) Å^3
Z = 18
$F(000)$ = 4186
D_x = 2.903 Mg m^{-3}
Mo $K\alpha$ radiation, λ = 0.71073 Å
Cell parameters from 4854 reflections
θ = 3.3–30.7°
μ = 2.10 mm^{-1}
T = 150 K
Plate, red orange
0.02 × 0.01 × 0.003 mm

Data collection

Bruker SMART APEXII three-circle diffractometer
Radiation source: X-ray tube
ω scans
Absorption correction: multi-scan (SADABS; Krause *et al.*, 2015)
T_{min} = 0.640, T_{max} = 0.746
15291 measured reflections
1108 independent reflections
892 reflections with $I > 2\sigma(I)$
R_{int} = 0.069
θ_{max} = 26.4°, θ_{min} = 3.3°
h = −26→26
k = −26→26
l = −15→15

Refinement

Refinement on F^2
Least-squares matrix: full
$R[F^2 > 2\sigma(F^2)]$ = 0.019
$wR(F^2)$ = 0.046
S = 1.01
1108 reflections
118 parameters
0 restraints
$w = 1/[\sigma^2(F_o^2) + (0.022P)^2]$ where $P = (F_o^2 + 2F_c^2)/3$
$(\Delta/\sigma)_{max} < 0.001$
$\Delta\rho_{max}$ = 0.37 e Å^{-3}
$\Delta\rho_{min}$ = −0.35 e Å^{-3}

Special details

Geometry. All esds (except the esd in the dihedral angle between two l.s. planes) are estimated using the full covariance matrix. The cell esds are taken into account individually in the estimation of esds in distances, angles and torsion angles; correlations between esds in cell parameters are only used when they are defined by crystal symmetry. An approximate (isotropic) treatment of cell esds is used for estimating esds involving l.s. planes.

Refinement. A thin plate exhibiting sharp extinction under cross polarized light was selected and mounted on a Mitegen cryoloop for the single crystal X-ray diffraction experiment at 150 (2) K. Data were collected using Mo *Kα* X-rays and an Apex II CCD-based detectormounted to a Bruker Smart Apex II three-circle diffractometer. Reflections were integrated and corrected for Lorentz, polarization, and background effects using the Bruker program SAINT. A multi-scan semi-empirical absorption correction was applied using equivalent reflections in SADABS-2015. An initial structure model was obtained by the charge-flipping method using SHELXT (Sheldrick, 2015a), and refinements were made by full-matrix least-squares on F^2 using SHELXL-2013 (Sheldrick, 2015b).

Fractional atomic coordinates and isotropic or equivalent isotropic displacement parameters (Å²)

	x	*y*	*z*	U_{iso}*/U_{eq}	Occ. (<1)
Fe1	0.6667	0.08597 (2)	0.0833	0.00531 (12)	
Si1	0.77731 (3)	0.01612 (3)	0.01782 (5)	0.00555 (15)	
Si2	0.90941 (3)	0.09550 (3)	−0.12341 (5)	0.00597 (14)	
Na1	1.0000	0.0000	−0.2500	0.0053 (4)	
Na2	1.0000	0.0000	0.0000	0.0091 (4)	
Na3	0.92352 (5)	0.06573 (5)	−0.36144 (7)	0.0119 (2)	
Na4	0.61847 (6)	−0.04819 (6)	−0.0833	0.0143 (3)	
Na5	0.8333	0.1667	0.1667	0.0318 (11)	0.682 (7)
Na51	0.8493 (4)	0.1771 (4)	0.0653 (13)	0.008 (3)*	0.144 (9)
Na52	0.8512 (3)	0.1796 (4)	0.0211 (14)	0.004 (3)*	0.145 (10)
Na53	0.840 (5)	0.168 (5)	−0.031 (11)	0.04 (3)*	0.017 (7)
O1	0.95460 (8)	0.05533 (8)	−0.13075 (13)	0.0122 (4)	
O2	0.73849 (8)	−0.02816 (8)	−0.08974 (13)	0.0097 (3)	
O3	0.85626 (8)	0.07936 (8)	−0.22531 (13)	0.0093 (3)	
O4	0.96207 (8)	0.18437 (8)	−0.11467 (13)	0.0094 (3)	
O5	0.86316 (8)	0.07307 (8)	−0.00744 (13)	0.0111 (4)	
O6	0.74346 (9)	0.05886 (9)	0.07485 (13)	0.0126 (4)	

Atomic displacement parameters (Å²)

	U^{11}	U^{22}	U^{33}	U^{12}	U^{13}	U^{23}
Fe1	0.0050 (2)	0.00458 (17)	0.0065 (2)	0.00249 (11)	0.00023 (18)	0.00011 (9)
Si1	0.0051 (3)	0.0058 (3)	0.0064 (3)	0.0032 (2)	0.0002 (2)	0.0006 (2)
Si2	0.0048 (3)	0.0050 (3)	0.0072 (3)	0.0018 (2)	−0.0008 (2)	−0.0005 (2)
Na1	0.0053 (6)	0.0053 (6)	0.0051 (10)	0.0027 (3)	0.000	0.000
Na2	0.0093 (7)	0.0093 (7)	0.0088 (11)	0.0046 (3)	0.000	0.000
Na3	0.0130 (5)	0.0099 (5)	0.0137 (5)	0.0065 (4)	0.0023 (4)	0.0013 (4)
Na4	0.0131 (5)	0.0131 (5)	0.0127 (7)	0.0035 (6)	0.0033 (3)	−0.0033 (3)
Na5	0.0230 (14)	0.0087 (12)	0.061 (2)	0.0058 (10)	−0.0258 (13)	−0.0051 (11)
O1	0.0104 (8)	0.0089 (8)	0.0177 (9)	0.0052 (7)	−0.0015 (7)	−0.0021 (7)
O2	0.0092 (8)	0.0085 (8)	0.0090 (9)	0.0026 (6)	−0.0007 (6)	0.0010 (6)
O3	0.0057 (8)	0.0088 (8)	0.0110 (9)	0.0016 (6)	−0.0014 (6)	−0.0005 (7)
O4	0.0103 (8)	0.0062 (8)	0.0081 (9)	0.0015 (7)	−0.0006 (6)	0.0003 (6)

O5	0.0067 (8)	0.0141 (9)	0.0088 (9)	0.0023 (7)	−0.0004 (6)	0.0002 (7)
O6	0.0158 (9)	0.0178 (9)	0.0118 (9)	0.0139 (8)	0.0011 (7)	0.0006 (7)

Geometric parameters (Å, º)

Fe1—O6	2.0021 (16)	Na4—O6^{xv}	2.4139 (16)
Fe1—O6^{i}	2.0022 (16)	Na4—O4^{xvi}	2.5162 (18)
Fe1—O3^{ii}	2.0333 (15)	Na4—O4^{xvii}	2.5163 (18)
Fe1—O3^{iii}	2.0334 (15)	Na4—Na51^{iv}	2.953 (7)
Fe1—O2^{iii}	2.0378 (16)	Na4—Na51^{xviii}	2.953 (7)
Fe1—O2^{ii}	2.0379 (16)	Na4—Na52^{iv}	2.996 (8)
Fe1—Na4	3.2486 (9)	Na4—Na52^{xviii}	2.996 (8)
Fe1—Na4^{ii}	3.2486 (9)	Na4—Si1^{i}	3.0967 (9)
Fe1—Na5	3.2572 (4)	Na4—Si1^{xv}	3.0968 (9)
Fe1—Na5^{i}	3.2572 (4)	Na5—Na51^{xix}	1.282 (16)
Fe1—Na51^{i}	3.395 (7)	Na5—Na51	1.282 (16)
Fe1—Na51	3.396 (7)	Na5—Na52	1.822 (17)
Si1—O6	1.5870 (16)	Na5—Na52^{xix}	1.822 (17)
Si1—O2	1.5968 (17)	Na5—O6^{xix}	2.4218 (18)
Si1—O5	1.6501 (17)	Na5—O6	2.4218 (17)
Si1—O4^{iv}	1.6635 (17)	Na5—Na53	2.43 (13)
Si1—Na53	2.89 (8)	Na5—Na53^{xix}	2.43 (13)
Si1—Na52	3.038 (7)	Na5—O3^{v}	2.5336 (16)
Si1—Na51	3.048 (7)	Na5—O3^{iii}	2.5336 (16)
Si1—Na4^{ii}	3.0968 (9)	Na5—O2^{xii}	2.7383 (16)
Si1—Na52^{iv}	3.136 (7)	Na5—O2^{ii}	2.7383 (16)
Si1—Na4	3.2140 (12)	Na51—Na52	0.546 (11)
Si1—Na53^{iv}	3.28 (9)	Na51—Na53	1.19 (13)
Si1—Na3^{v}	3.2908 (11)	Na51—O2^{xii}	2.295 (7)
Si2—O1	1.5868 (16)	Na51—O3^{iii}	2.359 (7)
Si2—O3	1.6095 (17)	Na51—O6	2.414 (7)
Si2—O4	1.6614 (16)	Na51—Na53^{iii}	2.49 (13)
Si2—O5	1.6636 (18)	Na51—O5	2.552 (8)
Si2—Na53^{iii}	2.84 (8)	Na51—Na51^{xix}	2.56 (3)
Si2—Na53	2.86 (9)	Na51—O4^{iii}	2.899 (11)
Si2—Na52^{iii}	2.944 (8)	Na51—Na4^{xii}	2.953 (7)
Si2—Na3	3.0413 (11)	Na52—Na53	0.68 (13)
Si2—Na3^{vi}	3.0601 (12)	Na52—Na53^{iii}	1.96 (13)
Si2—Na51^{iii}	3.141 (9)	Na52—O2^{xii}	2.396 (9)
Si2—Na52	3.194 (11)	Na52—O3^{iii}	2.411 (7)
Si2—Na3^{vii}	3.2032 (12)	Na52—O5	2.446 (7)
Na1—O1^{viii}	2.3770 (15)	Na52—O6	2.546 (8)
Na1—O1	2.3771 (15)	Na52—Na52^{iii}	2.57 (3)
Na1—O1^{vi}	2.3771 (15)	Na52—O4^{iii}	2.639 (8)
Na1—O1^{ix}	2.3771 (15)	Na52—O4	2.862 (11)
Na1—O1^{x}	2.3771 (15)	Na52—Si2^{iii}	2.944 (8)
Na1—O1^{vii}	2.3771 (15)	Na53—Na53^{iii}	1.3 (3)
Na1—Na3	2.9745 (9)	Na53—Na52^{iii}	1.96 (13)

Na1—Na3^{vii}	2.9746 (9)	Na53—O5	2.33 (8)
Na1—Na3^{ix}	2.9746 (9)	Na53—Na51^{iii}	2.49 (13)
Na1—Na3^{x}	2.9746 (9)	Na53—O3^{iii}	2.54 (9)
Na1—Na3^{vi}	2.9746 (9)	Na53—O6	2.57 (8)
Na1—Na3^{viii}	2.9746 (9)	Na53—O4^{iii}	2.64 (8)
Na2—O1^{xi}	2.4667 (16)	Na53—O4	2.66 (8)
Na2—O1^{xii}	2.4668 (16)	Na53—Si2^{iii}	2.84 (8)
Na2—O1^{ix}	2.4668 (16)	O1—Na3^{vii}	2.3300 (18)
Na2—O1	2.4668 (16)	O1—Na3^{vi}	2.3783 (18)
Na2—O1^{iv}	2.4668 (16)	O2—Fe1^{xv}	2.0378 (16)
Na2—O1^{x}	2.4668 (16)	O2—Na51^{iv}	2.295 (7)
Na2—Na1^{xi}	3.0728 (5)	O2—Na52^{iv}	2.396 (9)
Na2—Na3^{vi}	3.1421 (9)	O2—Na5^{xv}	2.7383 (16)
Na2—Na3^{xiii}	3.1421 (9)	O2—Na53^{iv}	2.85 (12)
Na2—Na3^{v}	3.1421 (9)	O3—Fe1^{xv}	2.0333 (15)
Na2—Na3^{viii}	3.1421 (9)	O3—Na51^{iii}	2.359 (7)
Na3—O3	2.3195 (18)	O3—Na52^{iii}	2.411 (7)
Na3—O1^{vii}	2.3299 (18)	O3—Na5^{iii}	2.5336 (16)
Na3—O5^{xiv}	2.3311 (18)	O3—Na53^{iii}	2.54 (9)
Na3—O1^{vi}	2.3781 (18)	O4—Si1^{xii}	1.6634 (17)
Na3—O1	2.9462 (19)	O4—Na4^{xx}	2.5162 (18)
Na3—O4^{vii}	3.0198 (18)	O4—Na53^{iii}	2.64 (8)
Na3—Si2^{vi}	3.0601 (12)	O4—Na52^{iii}	2.639 (8)
Na3—Na2^{viii}	3.1420 (9)	O4—Na51^{iii}	2.899 (11)
Na3—Si2^{vii}	3.2032 (12)	O4—Na3^{vii}	3.0198 (18)
Na3—Si1^{xiv}	3.2908 (11)	O5—Na3^{v}	2.3310 (18)
Na4—O2	2.3864 (18)	O5—Na53^{iii}	2.97 (10)
Na4—O2^{iii}	2.3865 (18)	O6—Na4^{ii}	2.4139 (16)
Na4—O6^{i}	2.4138 (16)		

O6—Fe1—O6^{i}	91.02 (10)	Na51^{xviii}—Na4—Na52^{iv}	157.39 (16)
O6—Fe1—O3^{ii}	174.17 (6)	O2—Na4—Na52^{xviii}	146.93 (19)
O6^{i}—Fe1—O3^{ii}	87.09 (7)	O2^{iii}—Na4—Na52^{xviii}	51.36 (15)
O6—Fe1—O3^{iii}	87.09 (7)	O6^{i}—Na4—Na52^{xviii}	78.4 (3)
O6^{i}—Fe1—O3^{iii}	174.17 (6)	O6^{xv}—Na4—Na52^{xviii}	101.8 (3)
O3^{ii}—Fe1—O3^{iii}	95.32 (9)	O4^{xvi}—Na4—Na52^{xviii}	56.4 (2)
O6—Fe1—O2^{iii}	97.56 (6)	O4^{xvii}—Na4—Na52^{xviii}	108.5 (2)
O6^{i}—Fe1—O2^{iii}	82.39 (6)	Na51^{iv}—Na4—Na52^{xviii}	157.40 (16)
O3^{ii}—Fe1—O2^{iii}	87.66 (6)	Na51^{xviii}—Na4—Na52^{xviii}	10.5 (2)
O3^{iii}—Fe1—O2^{iii}	92.39 (6)	Na52^{iv}—Na4—Na52^{xviii}	160.4 (2)
O6—Fe1—O2^{ii}	82.39 (6)	O2—Na4—Si1^{i}	109.99 (4)
O6^{i}—Fe1—O2^{ii}	97.56 (6)	O2^{iii}—Na4—Si1^{i}	97.53 (4)
O3^{ii}—Fe1—O2^{ii}	92.39 (6)	O6^{i}—Na4—Si1^{i}	30.37 (4)
O3^{iii}—Fe1—O2^{ii}	87.66 (6)	O6^{xv}—Na4—Si1^{i}	150.26 (6)
O2^{iii}—Fe1—O2^{ii}	179.92 (9)	O4^{xvi}—Na4—Si1^{i}	108.68 (6)
O6—Fe1—Na4	69.78 (5)	O4^{xvii}—Na4—Si1^{i}	32.43 (4)
O6^{i}—Fe1—Na4	47.81 (5)	Na51^{iv}—Na4—Si1^{i}	87.7 (3)
O3^{ii}—Fe1—Na4	112.56 (5)	Na51^{xviii}—Na4—Si1^{i}	84.7 (3)

O3^{iii}—Fe1—Na4	126.43 (5)	Na52^{iv}—Na4—Si1^{i}	78.0 (3)
O2^{iii}—Fe1—Na4	47.11 (5)	Na52^{xviii}—Na4—Si1^{i}	94.6 (3)
O2^{ii}—Fe1—Na4	132.81 (5)	O2—Na4—Si1^{xv}	97.52 (4)
O6—Fe1—Na4^{ii}	47.82 (5)	O2^{iii}—Na4—Si1^{xv}	109.99 (4)
O6^{i}—Fe1—Na4^{ii}	69.78 (5)	O6^{i}—Na4—Si1^{xv}	150.26 (6)
O3^{ii}—Fe1—Na4^{ii}	126.43 (5)	O6^{xv}—Na4—Si1^{xv}	30.37 (4)
O3^{iii}—Fe1—Na4^{ii}	112.56 (5)	O4^{xvi}—Na4—Si1^{xv}	32.43 (4)
O2^{iii}—Fe1—Na4^{ii}	132.81 (5)	O4^{xvii}—Na4—Si1^{xv}	108.68 (6)
O2^{ii}—Fe1—Na4^{ii}	47.11 (5)	Na51^{iv}—Na4—Si1^{xv}	84.7 (3)
Na4—Fe1—Na4^{ii}	86.946 (16)	Na51^{xviii}—Na4—Si1^{xv}	87.7 (3)
O6—Fe1—Na5	47.85 (5)	Na52^{iv}—Na4—Si1^{xv}	94.6 (3)
O6^{i}—Fe1—Na5	130.29 (5)	Na52^{xviii}—Na4—Si1^{xv}	78.0 (3)
O3^{ii}—Fe1—Na5	130.68 (5)	Si1^{i}—Na4—Si1^{xv}	135.81 (5)
O3^{iii}—Fe1—Na5	51.06 (5)	Na51^{xix}—Na5—Na51	180.0
O2^{iii}—Fe1—Na5	123.17 (4)	Na51^{xix}—Na5—Na52	177.1 (4)
O2^{ii}—Fe1—Na5	56.83 (4)	Na51—Na5—Na52	2.9 (4)
Na4—Fe1—Na5	116.582 (17)	Na51^{xix}—Na5—Na52^{xix}	2.9 (4)
Na4^{ii}—Fe1—Na5	61.832 (15)	Na51—Na5—Na52^{xix}	177.1 (4)
O6—Fe1—Na5^{i}	130.30 (5)	Na52—Na5—Na52^{xix}	180.0
O6^{i}—Fe1—Na5^{i}	47.85 (5)	Na51^{xix}—Na5—O6^{xix}	74.3 (3)
O3^{ii}—Fe1—Na5^{i}	51.06 (5)	Na51—Na5—O6^{xix}	105.7 (3)
O3^{iii}—Fe1—Na5^{i}	130.68 (5)	Na52—Na5—O6^{xix}	107.8 (2)
O2^{iii}—Fe1—Na5^{i}	56.82 (4)	Na52^{xix}—Na5—O6^{xix}	72.2 (2)
O2^{ii}—Fe1—Na5^{i}	123.17 (4)	Na51^{xix}—Na5—O6	105.7 (3)
Na4—Fe1—Na5^{i}	61.832 (15)	Na51—Na5—O6	74.3 (3)
Na4^{ii}—Fe1—Na5^{i}	116.542 (17)	Na52—Na5—O6	72.2 (2)
Na5—Fe1—Na5^{i}	178.070 (16)	Na52^{xix}—Na5—O6	107.8 (2)
O6—Fe1—Na51^{i}	135.44 (12)	O6^{xix}—Na5—O6	180.0
O6^{i}—Fe1—Na51^{i}	44.42 (12)	Na51^{xix}—Na5—Na53	169 (2)
O3^{ii}—Fe1—Na51^{i}	43.00 (13)	Na51—Na5—Na53	11 (2)
O3^{iii}—Fe1—Na51^{i}	137.13 (12)	Na52—Na5—Na53	8 (2)
O2^{iii}—Fe1—Na51^{i}	78.9 (3)	Na52^{xix}—Na5—Na53	172 (2)
O2^{ii}—Fe1—Na51^{i}	101.1 (3)	O6^{xix}—Na5—Na53	116 (2)
Na4—Fe1—Na51^{i}	76.4 (2)	O6—Na5—Na53	64 (2)
Na4^{ii}—Fe1—Na51^{i}	103.45 (19)	Na51^{xix}—Na5—Na53^{xix}	11 (2)
Na5—Fe1—Na51^{i}	157.9 (3)	Na51—Na5—Na53^{xix}	169 (2)
Na5^{i}—Fe1—Na51^{i}	22.1 (3)	Na52—Na5—Na53^{xix}	172 (2)
O6—Fe1—Na51	44.42 (12)	Na52^{xix}—Na5—Na53^{xix}	8 (2)
O6^{i}—Fe1—Na51	135.44 (12)	O6^{xix}—Na5—Na53^{xix}	64 (2)
O3^{ii}—Fe1—Na51	137.14 (12)	O6—Na5—Na53^{xix}	116 (2)
O3^{iii}—Fe1—Na51	43.00 (13)	Na53—Na5—Na53^{xix}	180.0
O2^{iii}—Fe1—Na51	101.1 (3)	Na51^{xix}—Na5—O3^{v}	67.4 (3)
O2^{ii}—Fe1—Na51	78.9 (3)	Na51—Na5—O3^{v}	112.6 (3)
Na4—Fe1—Na51	103.45 (19)	Na52—Na5—O3^{v}	115.2 (2)
Na4^{ii}—Fe1—Na51	76.5 (2)	Na52^{xix}—Na5—O3^{v}	64.8 (2)
Na5—Fe1—Na51	22.1 (3)	O6^{xix}—Na5—O3^{v}	68.21 (5)
Na5^{i}—Fe1—Na51	157.9 (3)	O6—Na5—O3^{v}	111.79 (5)
Na51^{i}—Fe1—Na51	179.9 (2)	Na53—Na5—O3^{v}	118.5 (19)

O6—Si1—O2	117.13 (9)	Na53^{xix}—Na5—O3^{v}	61.5 (19)
O6—Si1—O5	108.56 (9)	Na51^{xix}—Na5—O3^{iii}	112.6 (3)
O2—Si1—O5	109.88 (9)	Na51—Na5—O3^{iii}	67.4 (3)
O6—Si1—O4^{iv}	104.36 (9)	Na52—Na5—O3^{iii}	64.8 (2)
O2—Si1—O4^{iv}	111.19 (9)	Na52^{xix}—Na5—O3^{iii}	115.2 (2)
O5—Si1—O4^{iv}	104.93 (8)	O6^{xix}—Na5—O3^{iii}	111.79 (5)
O6—Si1—Na53	62.2 (19)	O6—Na5—O3^{iii}	68.21 (5)
O2—Si1—Na53	108 (3)	Na53—Na5—O3^{iii}	61.5 (19)
O5—Si1—Na53	53.7 (16)	Na53^{xix}—Na5—O3^{iii}	118.5 (19)
O4^{iv}—Si1—Na53	140 (3)	O3^{v}—Na5—O3^{iii}	180.0
O6—Si1—Na52	56.9 (2)	Na51^{xix}—Na5—O2^{xii}	123.5 (3)
O2—Si1—Na52	120.8 (3)	Na51—Na5—O2^{xii}	56.5 (3)
O5—Si1—Na52	53.47 (14)	Na52—Na5—O2^{xii}	59.4 (2)
O4^{iv}—Si1—Na52	127.7 (3)	Na52^{xix}—Na5—O2^{xii}	120.6 (2)
Na53—Si1—Na52	13 (3)	O6^{xix}—Na5—O2^{xii}	61.72 (5)
O6—Si1—Na51	51.81 (19)	O6—Na5—O2^{xii}	118.28 (5)
O2—Si1—Na51	130.5 (3)	Na53—Na5—O2^{xii}	67 (2)
O5—Si1—Na51	56.85 (17)	Na53^{xix}—Na5—O2^{xii}	113 (2)
O4^{iv}—Si1—Na51	118.3 (3)	O3^{v}—Na5—O2^{xii}	64.53 (5)
Na53—Si1—Na51	23 (3)	O3^{iii}—Na5—O2^{xii}	115.47 (5)
Na52—Si1—Na51	10.3 (2)	Na51^{xix}—Na5—O2^{ii}	56.5 (3)
O6—Si1—Na4^{ii}	50.28 (6)	Na51—Na5—O2^{ii}	123.5 (3)
O2—Si1—Na4^{ii}	128.99 (7)	Na52—Na5—O2^{ii}	120.6 (2)
O5—Si1—Na4^{ii}	121.02 (6)	Na52^{xix}—Na5—O2^{ii}	59.4 (2)
O4^{iv}—Si1—Na4^{ii}	54.21 (6)	O6^{xix}—Na5—O2^{ii}	118.27 (5)
Na53—Si1—Na4^{ii}	104 (2)	O6—Na5—O2^{ii}	61.72 (5)
Na52—Si1—Na4^{ii}	93.6 (3)	Na53—Na5—O2^{ii}	113 (2)
Na51—Si1—Na4^{ii}	84.0 (3)	Na53^{xix}—Na5—O2^{ii}	67 (2)
O6—Si1—Na52^{iv}	115.86 (18)	O3^{v}—Na5—O2^{ii}	115.47 (5)
O2—Si1—Na52^{iv}	48.4 (3)	O3^{iii}—Na5—O2^{ii}	64.53 (5)
O5—Si1—Na52^{iv}	135.58 (18)	O2^{xii}—Na5—O2^{ii}	180.0
O4^{iv}—Si1—Na52^{iv}	65.0 (3)	Na52—Na51—Na53	14 (4)
Na53—Si1—Na52^{iv}	155 (2)	Na52—Na51—Na5	170.1 (14)
Na52—Si1—Na52^{iv}	165.25 (15)	Na53—Na51—Na5	158 (4)
Na51—Si1—Na52^{iv}	167.25 (16)	Na52—Na51—O2^{xii}	94.1 (13)
Na4^{ii}—Si1—Na52^{iv}	89.2 (3)	Na53—Na51—O2^{xii}	105 (4)
O6—Si1—Na4	74.17 (7)	Na5—Na51—O2^{xii}	95.7 (6)
O2—Si1—Na4	45.57 (6)	Na52—Na51—O3^{iii}	88.9 (12)
O5—Si1—Na4	142.52 (7)	Na53—Na51—O3^{iii}	84 (4)
O4^{iv}—Si1—Na4	110.55 (6)	Na5—Na51—O3^{iii}	82.5 (4)
Na53—Si1—Na4	102 (2)	O2^{xii}—Na51—O3^{iii}	146.7 (3)
Na52—Si1—Na4	109.19 (18)	Na52—Na51—O6	97.8 (13)
Na51—Si1—Na4	112.80 (15)	Na53—Na51—O6	84 (4)
Na4^{ii}—Si1—Na4	90.18 (2)	Na5—Na51—O6	75.0 (4)
Na52^{iv}—Si1—Na4	56.28 (17)	O2^{xii}—Na51—O6	140.5 (4)
O6—Si1—Na53^{iv}	113.1 (15)	O3^{iii}—Na51—O6	71.24 (19)
O2—Si1—Na53^{iv}	60 (2)	Na52—Na51—Na53^{iii}	10 (2)
O5—Si1—Na53^{iv}	136.7 (14)	Na53—Na51—Na53^{iii}	7 (4)

O4^{iv}—Si1—Na53^{iv}	54 (2)	Na5—Na51—Na53^{iii}	160 (2)
Na53—Si1—Na53^{iv}	165.0 (19)	O2^{xii}—Na51—Na53^{iii}	104 (2)
Na52—Si1—Na53^{iv}	169.8 (14)	O3^{iii}—Na51—Na53^{iii}	82 (2)
Na51—Si1—Na53^{iv}	163.1 (18)	O6—Na51—Na53^{iii}	89 (2)
Na4^{ii}—Si1—Na53^{iv}	80 (2)	Na52—Na51—O5	72.7 (11)
Na52^{iv}—Si1—Na53^{iv}	12 (2)	Na53—Na51—O5	66 (4)
Na4—Si1—Na53^{iv}	63.6 (19)	Na5—Na51—O5	109.0 (5)
O6—Si1—Na3^{v}	104.22 (7)	O2^{xii}—Na51—O5	84.4 (2)
O2—Si1—Na3^{v}	137.13 (7)	O3^{iii}—Na51—O5	127.7 (4)
O5—Si1—Na3^{v}	41.62 (6)	O6—Na51—O5	63.84 (17)
O4^{iv}—Si1—Na3^{v}	65.86 (6)	Na53^{iii}—Na51—O5	72.2 (19)
Na53—Si1—Na3^{v}	81 (2)	Na52—Na51—Na51^{xix}	170.1 (14)
Na52—Si1—Na3^{v}	72.56 (19)	Na53—Na51—Na51^{xix}	158 (4)
Na51—Si1—Na3^{v}	68.25 (16)	Na5—Na51—Na51^{xix}	0.003 (1)
Na4^{ii}—Si1—Na3^{v}	85.85 (3)	O2^{xii}—Na51—Na51^{xix}	95.7 (6)
Na52^{iv}—Si1—Na3^{v}	122.13 (18)	O3^{iii}—Na51—Na51^{xix}	82.5 (4)
Na4—Si1—Na3^{v}	175.78 (3)	O6—Na51—Na51^{xix}	75.0 (4)
Na53^{iv}—Si1—Na3^{v}	114 (2)	Na53^{iii}—Na51—Na51^{xix}	160 (2)
O1—Si2—O3	113.39 (9)	O5—Na51—Na51^{xix}	109.0 (5)
O1—Si2—O4	112.09 (8)	Na52—Na51—O4^{iii}	56.6 (11)
O3—Si2—O4	107.36 (9)	Na53—Na51—O4^{iii}	65 (4)
O1—Si2—O5	109.19 (9)	Na5—Na51—O4^{iii}	121.4 (4)
O3—Si2—O5	110.47 (9)	O2^{xii}—Na51—O4^{iii}	95.5 (3)
O4—Si2—O5	103.92 (8)	O3^{iii}—Na51—O4^{iii}	59.1 (2)
O1—Si2—Na53^{iii}	173 (3)	O6—Na51—O4^{iii}	122.4 (4)
O3—Si2—Na53^{iii}	62 (2)	Na53^{iii}—Na51—O4^{iii}	58 (2)
O4—Si2—Na53^{iii}	65.6 (18)	O5—Na51—O4^{iii}	129.2 (6)
O5—Si2—Na53^{iii}	78 (3)	Na51^{xix}—Na51—O4^{iii}	121.4 (4)
O1—Si2—Na53	160 (3)	Na52—Na51—Na4^{xii}	89.3 (13)
O3—Si2—Na53	86 (3)	Na53—Na51—Na4^{xii}	103 (4)
O4—Si2—Na53	65.9 (18)	Na5—Na51—Na4^{xii}	96.2 (5)
O5—Si2—Na53	54.6 (19)	O2^{xii}—Na51—Na4^{xii}	52.29 (14)
Na53^{iii}—Si2—Na53	27 (5)	O3^{iii}—Na51—Na4^{xii}	94.7 (2)
O1—Si2—Na52^{iii}	159.7 (3)	O6—Na51—Na4^{xii}	164.0 (4)
O3—Si2—Na52^{iii}	54.9 (3)	Na53^{iii}—Na51—Na4^{xii}	97 (2)
O4—Si2—Na52^{iii}	62.86 (15)	O5—Na51—Na4^{xii}	132.1 (3)
O5—Si2—Na52^{iii}	91.0 (3)	Na51^{xix}—Na51—Na4^{xii}	96.2 (5)
Na53^{iii}—Si2—Na52^{iii}	13 (3)	O4^{iii}—Na51—Na4^{xii}	50.92 (14)
Na53—Si2—Na52^{iii}	39 (3)	Na52—Na51—Si1	83.8 (12)
O1—Si2—Na3	71.35 (6)	Na53—Na51—Si1	71 (4)
O3—Si2—Na3	48.71 (6)	Na5—Na51—Si1	92.8 (4)
O4—Si2—Na3	102.75 (6)	O2^{xii}—Na51—Si1	114.7 (2)
O5—Si2—Na3	150.56 (7)	O3^{iii}—Na51—Si1	98.6 (2)
Na53^{iii}—Si2—Na3	102 (3)	O6—Na51—Si1	31.11 (9)
Na53—Si2—Na3	129 (2)	Na53^{iii}—Na51—Si1	78 (2)
Na52^{iii}—Si2—Na3	90.2 (3)	O5—Na51—Si1	32.77 (9)
O1—Si2—Na3^{vi}	50.13 (6)	Na51^{xix}—Na51—Si1	92.8 (4)
O3—Si2—Na3^{vi}	83.84 (6)	O4^{iii}—Na51—Si1	132.2 (5)

O4—Si2—Na3^{vi}	162.21 (6)	Na4^{xii}—Na51—Si1	164.9 (4)
O5—Si2—Na3^{vi}	84.22 (6)	Na51—Na52—Na53	154 (7)
Na53^{iii}—Si2—Na3^{vi}	132.1 (17)	Na51—Na52—Na5	6.9 (10)
Na53—Si2—Na3^{vi}	130.1 (17)	Na53—Na52—Na5	149 (7)
Na52^{iii}—Si2—Na3^{vi}	133.69 (16)	Na51—Na52—Na53^{iii}	167 (3)
Na3—Si2—Na3^{vi}	73.90 (3)	Na53—Na52—Na53^{iii}	15 (6)
O1—Si2—Na51^{iii}	150.9 (3)	Na5—Na52—Na53^{iii}	161 (3)
O3—Si2—Na51^{iii}	47.0 (2)	Na51—Na52—O2^{xii}	72.8 (13)
O4—Si2—Na51^{iii}	66.15 (17)	Na53—Na52—O2^{xii}	126 (7)
O5—Si2—Na51^{iii}	99.0 (2)	Na5—Na52—O2^{xii}	79.7 (5)
Na53^{iii}—Si2—Na51^{iii}	22 (3)	Na53^{iii}—Na52—O2^{xii}	120 (3)
Na53—Si2—Na51^{iii}	49 (2)	Na51—Na52—O3^{iii}	78.1 (11)
Na52^{iii}—Si2—Na51^{iii}	9.6 (2)	Na53—Na52—O3^{iii}	93 (7)
Na3—Si2—Na51^{iii}	80.6 (3)	Na5—Na52—O3^{iii}	72.0 (4)
Na3^{vi}—Si2—Na51^{iii}	128.93 (18)	Na53^{iii}—Na52—O3^{iii}	93 (2)
O1—Si2—Na52	148.6 (3)	O2^{xii}—Na52—O3^{iii}	136.1 (6)
O3—Si2—Na52	96.9 (3)	Na51—Na52—O5	95.0 (12)
O4—Si2—Na52	63.29 (14)	Na53—Na52—O5	72 (7)
O5—Si2—Na52	48.9 (2)	Na5—Na52—O5	96.3 (4)
Na53^{iii}—Si2—Na52	37 (3)	Na53^{iii}—Na52—O5	84 (2)
Na53—Si2—Na52	11 (2)	O2^{xii}—Na52—O5	84.7 (2)
Na52^{iii}—Si2—Na52	49.4 (6)	O3^{iii}—Na52—O5	130.4 (3)
Na3—Si2—Na52	139.5 (3)	Na51—Na52—O6	69.9 (11)
Na3^{vi}—Si2—Na52	130.37 (16)	Na53—Na52—O6	84 (7)
Na51^{iii}—Si2—Na52	58.9 (5)	Na5—Na52—O6	64.9 (3)
O1—Si2—Na3^{vii}	43.70 (6)	Na53^{iii}—Na52—O6	99 (3)
O3—Si2—Na3^{vii}	125.56 (7)	O2^{xii}—Na52—O6	127.5 (5)
O4—Si2—Na3^{vii}	68.50 (6)	O3^{iii}—Na52—O6	68.2 (2)
O5—Si2—Na3^{vii}	123.43 (6)	O5—Na52—O6	63.50 (17)
Na53^{iii}—Si2—Na3^{vii}	133 (2)	Na51—Na52—Na52^{iii}	174.4 (13)
Na53—Si2—Na3^{vii}	131 (2)	Na53—Na52—Na52^{iii}	21 (7)
Na52^{iii}—Si2—Na3^{vii}	125.81 (16)	Na5—Na52—Na52^{iii}	167.5 (3)
Na3—Si2—Na3^{vii}	78.29 (3)	Na53^{iii}—Na52—Na52^{iii}	7 (3)
Na3^{vi}—Si2—Na3^{vii}	93.78 (3)	O2^{xii}—Na52—Na52^{iii}	112.8 (4)
Na51^{iii}—Si2—Na3^{vii}	123.48 (14)	O3^{iii}—Na52—Na52^{iii}	97.4 (5)
Na52—Si2—Na3^{vii}	123.12 (15)	O5—Na52—Na52^{iii}	85.4 (5)
O1^{viii}—Na1—O1	174.87 (8)	O6—Na52—Na52^{iii}	105.4 (4)
O1^{viii}—Na1—O1^{vi}	85.97 (6)	Na51—Na52—O4^{iii}	113.4 (13)
O1—Na1—O1^{vi}	97.65 (8)	Na53—Na52—O4^{iii}	82 (7)
O1^{viii}—Na1—O1^{ix}	97.65 (8)	Na5—Na52—O4^{iii}	112.3 (4)
O1—Na1—O1^{ix}	85.97 (6)	Na53^{iii}—Na52—O4^{iii}	69 (2)
O1^{vi}—Na1—O1^{ix}	90.65 (8)	O2^{xii}—Na52—O4^{iii}	100.2 (2)
O1^{viii}—Na1—O1^{x}	90.65 (8)	O3^{iii}—Na52—O4^{iii}	62.73 (16)
O1—Na1—O1^{x}	85.97 (6)	O5—Na52—O4^{iii}	151.4 (7)
O1^{vi}—Na1—O1^{x}	174.87 (8)	O6—Na52—O4^{iii}	128.1 (3)
O1^{ix}—Na1—O1^{x}	85.97 (6)	Na52^{iii}—Na52—O4^{iii}	66.6 (4)
O1^{viii}—Na1—O1^{vii}	85.97 (6)	Na51—Na52—O4	127.0 (12)
O1—Na1—O1^{vii}	90.65 (8)	Na53—Na52—O4	66 (7)

O1^{vi}—Na1—O1^{vii}	85.97 (6)	Na5—Na52—O4	133.2 (4)
O1^{ix}—Na1—O1^{vii}	174.87 (8)	Na53^{iii}—Na52—O4	63 (3)
O1^{x}—Na1—O1^{vii}	97.66 (8)	O2^{xii}—Na52—O4	60.77 (17)
O1^{viii}—Na1—Na3	114.51 (4)	O3^{iii}—Na52—O4	154.7 (7)
O1—Na1—Na3	65.71 (4)	O5—Na52—O4	58.5 (2)
O1^{vi}—Na1—Na3	51.29 (4)	O6—Na52—O4	120.1 (3)
O1^{ix}—Na1—Na3	124.81 (4)	Na52^{iii}—Na52—O4	57.8 (4)
O1^{x}—Na1—Na3	133.81 (4)	O4^{iii}—Na52—O4	99.2 (4)
O1^{vii}—Na1—Na3	50.11 (4)	Na51—Na52—Si2^{iii}	106.3 (12)
O1^{viii}—Na1—Na3^{vii}	124.81 (4)	Na53—Na52—Si2^{iii}	75 (7)
O1—Na1—Na3^{vii}	50.11 (4)	Na5—Na52—Si2^{iii}	101.5 (4)
O1^{vi}—Na1—Na3^{vii}	133.81 (4)	Na53^{iii}—Na52—Si2^{iii}	68 (2)
O1^{ix}—Na1—Na3^{vii}	114.51 (4)	O2^{xii}—Na52—Si2^{iii}	131.7 (3)
O1^{x}—Na1—Na3^{vii}	51.30 (4)	O3^{iii}—Na52—Si2^{iii}	33.12 (11)
O1^{vii}—Na1—Na3^{vii}	65.71 (4)	O5—Na52—Si2^{iii}	141.7 (5)
Na3—Na1—Na3^{vii}	83.05 (4)	O6—Na52—Si2^{iii}	94.0 (2)
O1^{viii}—Na1—Na3^{ix}	51.30 (4)	Na52^{iii}—Na52—Si2^{iii}	70.4 (4)
O1—Na1—Na3^{ix}	133.81 (4)	O4^{iii}—Na52—Si2^{iii}	34.07 (10)
O1^{vi}—Na1—Na3^{ix}	50.11 (4)	O4—Na52—Si2^{iii}	122.9 (5)
O1^{ix}—Na1—Na3^{ix}	65.71 (4)	Na52—Na53—Na51	11 (4)
O1^{x}—Na1—Na3^{ix}	124.81 (4)	Na52—Na53—Na53^{iii}	157 (9)
O1^{vii}—Na1—Na3^{ix}	114.51 (4)	Na51—Na53—Na53^{iii}	167 (9)
Na3—Na1—Na3^{ix}	100.48 (2)	Na52—Na53—Na52^{iii}	151 (10)
Na3^{vii}—Na1—Na3^{ix}	175.56 (3)	Na51—Na53—Na52^{iii}	163 (7)
O1^{viii}—Na1—Na3^{x}	50.11 (4)	Na53^{iii}—Na53—Na52^{iii}	8 (4)
O1—Na1—Na3^{x}	124.81 (4)	Na52—Na53—O5	91 (8)
O1^{vi}—Na1—Na3^{x}	114.51 (4)	Na51—Na53—O5	86 (5)
O1^{ix}—Na1—Na3^{x}	133.81 (4)	Na53^{iii}—Na53—O5	106 (9)
O1^{x}—Na1—Na3^{x}	65.71 (4)	Na52^{iii}—Na53—O5	105 (5)
O1^{vii}—Na1—Na3^{x}	51.30 (4)	Na52—Na53—Na5	23 (5)
Na3—Na1—Na3^{x}	100.48 (2)	Na51—Na53—Na5	12 (2)
Na3^{vii}—Na1—Na3^{x}	76.12 (3)	Na53^{iii}—Na53—Na5	168 (9)
Na3^{ix}—Na1—Na3^{x}	100.48 (2)	Na52^{iii}—Na53—Na5	170 (5)
O1^{viii}—Na1—Na3^{vi}	133.81 (4)	O5—Na53—Na5	85 (3)
O1—Na1—Na3^{vi}	51.30 (4)	Na52—Na53—Na51^{iii}	154 (9)
O1^{vi}—Na1—Na3^{vi}	65.71 (4)	Na51—Na53—Na51^{iii}	165 (6)
O1^{ix}—Na1—Na3^{vi}	50.11 (4)	Na53^{iii}—Na53—Na51^{iii}	6 (4)
O1^{x}—Na1—Na3^{vi}	114.51 (4)	Na52^{iii}—Na53—Na51^{iii}	2.8 (7)
O1^{vii}—Na1—Na3^{vi}	124.81 (4)	O5—Na53—Na51^{iii}	103 (4)
Na3—Na1—Na3^{vi}	76.12 (3)	Na5—Na53—Na51^{iii}	172 (4)
Na3^{vii}—Na1—Na3^{vi}	100.48 (2)	Na52—Na53—O3^{iii}	72 (7)
Na3^{ix}—Na1—Na3^{vi}	83.05 (4)	Na51—Na53—O3^{iii}	68 (4)
Na3^{x}—Na1—Na3^{vi}	175.56 (3)	Na53^{iii}—Na53—O3^{iii}	107 (7)
O1^{viii}—Na1—Na3^{viii}	65.71 (4)	Na52^{iii}—Na53—O3^{iii}	112 (4)
O1—Na1—Na3^{viii}	114.51 (4)	O5—Na53—O3^{iii}	130 (4)
O1^{vi}—Na1—Na3^{viii}	124.81 (4)	Na5—Na53—O3^{iii}	61 (3)
O1^{ix}—Na1—Na3^{viii}	51.29 (4)	Na51^{iii}—Na53—O3^{iii}	112 (4)
O1^{x}—Na1—Na3^{viii}	50.11 (4)	Na52—Na53—O6	80 (7)

O1^{vii}—Na1—Na3^{viii}	133.81 (4)	Na51—Na53—O6	69 (4)
Na3—Na1—Na3^{viii}	175.56 (4)	Na53^{iii}—Na53—O6	121 (3)
Na3^{vii}—Na1—Na3^{viii}	100.48 (2)	Na52^{iii}—Na53—O6	128 (6)
Na3^{ix}—Na1—Na3^{viii}	76.12 (3)	O5—Na53—O6	65 (2)
Na3^{x}—Na1—Na3^{viii}	83.05 (4)	Na5—Na53—O6	58 (2)
Na3^{vi}—Na1—Na3^{viii}	100.48 (2)	Na51^{iii}—Na53—O6	125 (5)
O1^{xi}—Na2—O1^{xii}	82.15 (5)	O3^{iii}—Na53—O6	66 (2)
O1^{xi}—Na2—O1^{ix}	97.85 (5)	Na52—Na53—O4^{iii}	83 (8)
O1^{xii}—Na2—O1^{ix}	180.00 (8)	Na51—Na53—O4^{iii}	90 (5)
O1^{xi}—Na2—O1	180.0	Na53^{iii}—Na53—O4^{iii}	77 (6)
O1^{xii}—Na2—O1	97.85 (5)	Na52^{iii}—Na53—O4^{iii}	76 (3)
O1^{ix}—Na2—O1	82.15 (5)	O5—Na53—O4^{iii}	165 (4)
O1^{xi}—Na2—O1^{iv}	82.14 (5)	Na5—Na53—O4^{iii}	95 (4)
O1^{xii}—Na2—O1^{iv}	82.14 (5)	Na51^{iii}—Na53—O4^{iii}	78 (3)
O1^{ix}—Na2—O1^{iv}	97.86 (5)	O3^{iii}—Na53—O4^{iii}	61.2 (19)
O1—Na2—O1^{iv}	97.85 (5)	O6—Na53—O4^{iii}	127 (3)
O1^{xi}—Na2—O1^{x}	97.86 (5)	Na52—Na53—O4	101 (8)
O1^{xii}—Na2—O1^{x}	97.86 (5)	Na51—Na53—O4	107 (6)
O1^{ix}—Na2—O1^{x}	82.14 (5)	Na53^{iii}—Na53—O4	75 (7)
O1—Na2—O1^{x}	82.15 (5)	Na52^{iii}—Na53—O4	68 (3)
O1^{iv}—Na2—O1^{x}	180.00 (8)	O5—Na53—O4	63 (2)
O1^{xi}—Na2—Na1^{xi}	49.34 (4)	Na5—Na53—O4	116 (4)
O1^{xii}—Na2—Na1^{xi}	49.35 (4)	Na51^{iii}—Na53—O4	68 (3)
O1^{ix}—Na2—Na1^{xi}	130.65 (4)	O3^{iii}—Na53—O4	164 (4)
O1—Na2—Na1^{xi}	130.65 (4)	O6—Na53—O4	128 (3)
O1^{iv}—Na2—Na1^{xi}	49.35 (4)	O4^{iii}—Na53—O4	105 (3)
O1^{x}—Na2—Na1^{xi}	130.65 (4)	Na52—Na53—Si2^{iii}	92 (8)
O1^{xi}—Na2—Na1	130.66 (4)	Na51—Na53—Si2^{iii}	93 (5)
O1^{xii}—Na2—Na1	130.65 (4)	Na53^{iii}—Na53—Si2^{iii}	78 (7)
O1^{ix}—Na2—Na1	49.35 (4)	Na52^{iii}—Na53—Si2^{iii}	81 (3)
O1—Na2—Na1	49.35 (4)	O5—Na53—Si2^{iii}	159 (4)
O1^{iv}—Na2—Na1	130.65 (4)	Na5—Na53—Si2^{iii}	91 (3)
O1^{x}—Na2—Na1	49.35 (4)	Na51^{iii}—Na53—Si2^{iii}	82 (3)
Na1^{xi}—Na2—Na1	180.0	O3^{iii}—Na53—Si2^{iii}	34.2 (10)
O1^{xi}—Na2—Na3^{vi}	131.65 (4)	O6—Na53—Si2^{iii}	96 (3)
O1^{xii}—Na2—Na3^{vi}	132.78 (4)	O4^{iii}—Na53—Si2^{iii}	35.1 (10)
O1^{ix}—Na2—Na3^{vi}	47.22 (4)	O4—Na53—Si2^{iii}	136 (3)
O1—Na2—Na3^{vi}	48.35 (4)	Si2—O1—Na3^{vii}	108.23 (8)
O1^{iv}—Na2—Na3^{vi}	73.48 (4)	Si2—O1—Na1	144.87 (9)
O1^{x}—Na2—Na3^{vi}	106.52 (4)	Na3^{vii}—O1—Na1	78.38 (5)
Na1^{xi}—Na2—Na3^{vi}	122.822 (17)	Si2—O1—Na3^{vi}	99.07 (8)
Na1—Na2—Na3^{vi}	57.178 (17)	Na3^{vii}—O1—Na3^{vi}	152.51 (8)
O1^{xi}—Na2—Na3^{xiii}	48.35 (4)	Na1—O1—Na3^{vi}	77.44 (5)
O1^{xii}—Na2—Na3^{xiii}	47.22 (4)	Si2—O1—Na2	135.83 (9)
O1^{ix}—Na2—Na3^{xiii}	132.78 (4)	Na3^{vii}—O1—Na2	81.79 (5)
O1—Na2—Na3^{xiii}	131.65 (4)	Na1—O1—Na2	78.72 (5)
O1^{iv}—Na2—Na3^{xiii}	106.52 (4)	Na3^{vi}—O1—Na2	80.84 (5)
O1^{x}—Na2—Na3^{xiii}	73.48 (4)	Si2—O1—Na3	77.97 (6)

Na1^{xi}—Na2—Na3^{xiii}	57.178 (17)	Na3^{vii}—O1—Na3	96.04 (6)
Na1—Na2—Na3^{xiii}	122.822 (17)	Na1—O1—Na3	66.96 (4)
Na3^{vi}—Na2—Na3^{xiii}	180.00 (4)	Na3^{vi}—O1—Na3	86.38 (6)
O1^{xi}—Na2—Na3^{v}	106.52 (4)	Na2—O1—Na3	145.24 (6)
O1^{xii}—Na2—Na3^{v}	48.35 (4)	Si1—O2—Fe1^{xv}	131.94 (9)
O1^{ix}—Na2—Na3^{v}	131.65 (4)	Si1—O2—Na51^{iv}	114.3 (4)
O1—Na2—Na3^{v}	73.48 (4)	Fe1^{xv}—O2—Na51^{iv}	112.4 (4)
O1^{iv}—Na2—Na3^{v}	47.22 (4)	Si1—O2—Na4	105.88 (8)
O1^{x}—Na2—Na3^{v}	132.78 (4)	Fe1^{xv}—O2—Na4	94.16 (6)
Na1^{xi}—Na2—Na3^{v}	57.178 (17)	Na51^{iv}—O2—Na4	78.18 (17)
Na1—Na2—Na3^{v}	122.822 (17)	Si1—O2—Na52^{iv}	101.7 (4)
Na3^{vi}—Na2—Na3^{v}	86.60 (2)	Fe1^{xv}—O2—Na52^{iv}	125.4 (4)
Na3^{xiii}—Na2—Na3^{v}	93.40 (2)	Na51^{iv}—O2—Na52^{iv}	13.1 (3)
O1^{xi}—Na2—Na3^{viii}	73.48 (4)	Na4—O2—Na52^{iv}	77.56 (16)
O1^{xii}—Na2—Na3^{viii}	131.65 (4)	Si1—O2—Na5^{xv}	140.62 (9)
O1^{ix}—Na2—Na3^{viii}	48.35 (4)	Fe1^{xv}—O2—Na5^{xv}	84.65 (5)
O1—Na2—Na3^{viii}	106.52 (4)	Na51^{iv}—O2—Na5^{xv}	27.8 (4)
O1^{iv}—Na2—Na3^{viii}	132.78 (4)	Na4—O2—Na5^{xv}	81.11 (5)
O1^{x}—Na2—Na3^{viii}	47.22 (4)	Na52^{iv}—O2—Na5^{xv}	40.9 (4)
Na1^{xi}—Na2—Na3^{viii}	122.822 (17)	Si1—O2—Na53^{iv}	91 (2)
Na1—Na2—Na3^{viii}	57.178 (17)	Fe1^{xv}—O2—Na53^{iv}	136 (2)
Na3^{vi}—Na2—Na3^{viii}	93.40 (2)	Na51^{iv}—O2—Na53^{iv}	24 (2)
Na3^{xiii}—Na2—Na3^{viii}	86.60 (2)	Na4—O2—Na53^{iv}	81.2 (17)
Na3^{v}—Na2—Na3^{viii}	180.00 (4)	Na52^{iv}—O2—Na53^{iv}	11 (2)
O3—Na3—O1^{vii}	130.97 (7)	Na5^{xv}—O2—Na53^{iv}	51 (2)
O3—Na3—O5^{xiv}	106.96 (7)	Si2—O3—Fe1^{xv}	130.90 (9)
O1^{vii}—Na3—O5^{xiv}	95.39 (6)	Si2—O3—Na3	99.86 (8)
O3—Na3—O1^{vi}	110.83 (6)	Fe1^{xv}—O3—Na3	105.91 (7)
O1^{vii}—Na3—O1^{vi}	87.01 (8)	Si2—O3—Na51^{iii}	103.0 (4)
O5^{xiv}—Na3—O1^{vi}	126.84 (7)	Fe1^{xv}—O3—Na51^{iii}	101.0 (2)
O3—Na3—O1	59.56 (5)	Na3—O3—Na51^{iii}	117.5 (3)
O1^{vii}—Na3—O1	78.74 (6)	Si2—O3—Na52^{iii}	91.9 (3)
O5^{xiv}—Na3—O1	148.85 (6)	Fe1^{xv}—O3—Na52^{iii}	103.89 (17)
O1^{vi}—Na3—O1	83.73 (6)	Na3—O3—Na52^{iii}	127.3 (3)
O3—Na3—Na1	104.54 (5)	Na51^{iii}—O3—Na52^{iii}	13.1 (3)
O1^{vii}—Na3—Na1	51.51 (4)	Si2—O3—Na5^{iii}	128.80 (8)
O5^{xiv}—Na3—Na1	144.98 (5)	Fe1^{xv}—O3—Na5^{iii}	90.31 (6)
O1^{vi}—Na3—Na1	51.26 (4)	Na3—O3—Na5^{iii}	94.40 (6)
O1—Na3—Na1	47.34 (3)	Na51^{iii}—O3—Na5^{iii}	30.1 (4)
O3—Na3—O4^{vii}	98.08 (6)	Na52^{iii}—O3—Na5^{iii}	43.2 (4)
O1^{vii}—Na3—O4^{vii}	58.81 (5)	Si2—O3—Na53^{iii}	83 (2)
O5^{xiv}—Na3—O4^{vii}	57.09 (5)	Fe1^{xv}—O3—Na53^{iii}	100 (2)
O1^{vi}—Na3—O4^{vii}	145.13 (6)	Na3—O3—Na53^{iii}	142 (3)
O1—Na3—O4^{vii}	95.10 (5)	Na51^{iii}—O3—Na53^{iii}	28 (3)
Na1—Na3—O4^{vii}	103.72 (4)	Na52^{iii}—O3—Na53^{iii}	15 (3)
O3—Na3—Si2	31.43 (4)	Na5^{iii}—O3—Na53^{iii}	57 (3)
O1^{vii}—Na3—Si2	100.66 (5)	Si2—O4—Si1^{xii}	133.26 (10)
O5^{xiv}—Na3—Si2	125.28 (5)	Si2—O4—Na4^{xx}	133.09 (9)

O1^{vi}—Na3—Si2	106.08 (5)	Si1^{xii}—O4—Na4^{xx}	93.37 (7)
O1—Na3—Si2	30.68 (3)	Si2—O4—Na53^{iii}	79.3 (19)
Na1—Na3—Si2	78.01 (3)	Si1^{xii}—O4—Na53^{iii}	117 (2)
O4^{vii}—Na3—Si2	88.36 (4)	Na4^{xx}—O4—Na53^{iii}	83 (3)
O3—Na3—Si2^{vi}	90.67 (5)	Si2—O4—Na52^{iii}	83.07 (15)
O1^{vii}—Na3—Si2^{vi}	117.68 (5)	Si1^{xii}—O4—Na52^{iii}	124.6 (3)
O5^{xiv}—Na3—Si2^{vi}	116.49 (5)	Na4^{xx}—O4—Na52^{iii}	71.0 (3)
O1^{vi}—Na3—Si2^{vi}	30.80 (4)	Na53^{iii}—O4—Na52^{iii}	15 (3)
O1—Na3—Si2^{vi}	92.76 (4)	Si2—O4—Na53	79 (2)
Na1—Na3—Si2^{vi}	77.71 (2)	Si1^{xii}—O4—Na53	96 (3)
O4^{vii}—Na3—Si2^{vi}	170.38 (5)	Na4^{xx}—O4—Na53	104.2 (19)
Si2—Na3—Si2^{vi}	101.22 (3)	Na53^{iii}—O4—Na53	29 (6)
O3—Na3—Na2^{viii}	160.58 (5)	Na52^{iii}—O4—Na53	43 (3)
O1^{vii}—Na3—Na2^{viii}	50.99 (4)	Si2—O4—Na52	85.47 (15)
O5^{xiv}—Na3—Na2^{viii}	91.28 (5)	Si1^{xii}—O4—Na52	83.2 (3)
O1^{vi}—Na3—Na2^{viii}	50.81 (4)	Na4^{xx}—O4—Na52	108.8 (2)
O1—Na3—Na2^{viii}	107.43 (4)	Na53^{iii}—O4—Na52	41 (3)
Na1—Na3—Na2^{viii}	60.240 (19)	Na52^{iii}—O4—Na52	55.6 (6)
O4^{vii}—Na3—Na2^{viii}	97.44 (4)	Na53—O4—Na52	13 (3)
Si2—Na3—Na2^{viii}	138.08 (3)	Si2—O4—Na51^{iii}	82.25 (14)
Si2^{vi}—Na3—Na2^{viii}	74.87 (2)	Si1^{xii}—O4—Na51^{iii}	131.5 (2)
O3—Na3—Si2^{vii}	117.06 (5)	Na4^{xx}—O4—Na51^{iii}	65.63 (19)
O1^{vii}—Na3—Si2^{vii}	28.07 (4)	Na53^{iii}—O4—Na51^{iii}	24 (3)
O5^{xiv}—Na3—Si2^{vii}	76.82 (5)	Na52^{iii}—O4—Na51^{iii}	9.9 (3)
O1^{vi}—Na3—Si2^{vii}	114.97 (5)	Na53—O4—Na51^{iii}	53 (3)
O1—Na3—Si2^{vii}	85.01 (4)	Na52—O4—Na51^{iii}	65.5 (5)
Na1—Na3—Si2^{vii}	75.50 (2)	Si2—O4—Na3^{vii}	80.72 (6)
O4^{vii}—Na3—Si2^{vii}	30.79 (3)	Si1^{xii}—O4—Na3^{vii}	83.96 (7)
Si2—Na3—Si2^{vii}	94.32 (3)	Na4^{xx}—O4—Na3^{vii}	103.29 (6)
Si2^{vi}—Na3—Si2^{vii}	145.35 (3)	Na53^{iii}—O4—Na3^{vii}	157.6 (18)
Na2^{viii}—Na3—Si2^{vii}	72.91 (2)	Na52^{iii}—O4—Na3^{vii}	150.6 (3)
O3—Na3—Si1^{xiv}	98.52 (5)	Na53—O4—Na3^{vii}	152.5 (18)
O1^{vii}—Na3—Si1^{xiv}	81.26 (5)	Na52—O4—Na3^{vii}	146.0 (3)
O5^{xiv}—Na3—Si1^{xiv}	28.05 (4)	Na51^{iii}—O4—Na3^{vii}	141.5 (3)
O1^{vi}—Na3—Si1^{xiv}	148.84 (5)	Si1—O5—Si2	131.09 (10)
O1—Na3—Si1^{xiv}	121.54 (4)	Si1—O5—Na3^{v}	110.33 (8)
Na1—Na3—Si1^{xiv}	131.54 (3)	Si2—O5—Na3^{v}	111.42 (8)
O4^{vii}—Na3—Si1^{xiv}	30.18 (3)	Si1—O5—Na53	92 (2)
Si2—Na3—Si1^{xiv}	104.43 (3)	Si2—O5—Na53	90 (3)
Si2^{vi}—Na3—Si1^{xiv}	144.41 (4)	Na3^{v}—O5—Na53	119 (3)
Na2^{viii}—Na3—Si1^{xiv}	100.76 (3)	Si1—O5—Na52	93.71 (18)
Si2^{vii}—Na3—Si1^{xiv}	56.05 (2)	Si2—O5—Na52	100.3 (4)
O2—Na4—O2^{iii}	102.12 (9)	Na3^{v}—O5—Na52	103.4 (4)
O2—Na4—O6^{i}	112.10 (6)	Na53—O5—Na52	16 (3)
O2^{iii}—Na4—O6^{i}	67.32 (5)	Si1—O5—Na51	90.38 (19)
O2—Na4—O6^{xv}	67.32 (5)	Si2—O5—Na51	111.1 (3)
O2^{iii}—Na4—O6^{xv}	112.11 (6)	Na3^{v}—O5—Na51	93.6 (3)
O6^{i}—Na4—O6^{xv}	179.16 (10)	Na53—O5—Na51	28 (3)

O2—Na4—O4^{xvi}	129.28 (5)	Na52—O5—Na51	12.3 (3)
O2^{iii}—Na4—O4^{xvi}	104.01 (5)	Si1—O5—Na53^{iii}	94.6 (19)
O6^{i}—Na4—O4^{xvi}	117.92 (6)	Si2—O5—Na53^{iii}	69 (2)
O6^{xv}—Na4—O4^{xvi}	62.74 (5)	Na3^{v}—O5—Na53^{iii}	139.0 (16)
O2—Na4—O4^{xvii}	104.01 (5)	Na53—O5—Na53^{iii}	25 (5)
O2^{iii}—Na4—O4^{xvii}	129.28 (5)	Na52—O5—Na53^{iii}	41 (2)
O6^{i}—Na4—O4^{xvii}	62.75 (5)	Na51—O5—Na53^{iii}	53 (2)
O6^{xv}—Na4—O4^{xvii}	117.91 (6)	Si1—O6—Fe1	150.31 (11)
O4^{xvi}—Na4—O4^{xvii}	91.74 (8)	Si1—O6—Na4^{ii}	99.35 (8)
O2—Na4—Na51^{iv}	49.53 (13)	Fe1—O6—Na4^{ii}	94.26 (7)
O2^{iii}—Na4—Na51^{iv}	150.61 (15)	Si1—O6—Na51	97.1 (2)
O6^{i}—Na4—Na51^{iv}	112.2 (3)	Fe1—O6—Na51	100.09 (17)
O6^{xv}—Na4—Na51^{iv}	67.9 (3)	Na4^{ii}—O6—Na51	116.8 (4)
O4^{xvi}—Na4—Na51^{iv}	101.6 (2)	Si1—O6—Na5	112.41 (9)
O4^{xvii}—Na4—Na51^{iv}	63.4 (2)	Fe1—O6—Na5	94.35 (6)
O2—Na4—Na51^{xviii}	150.60 (15)	Na4^{ii}—O6—Na5	87.45 (5)
O2^{iii}—Na4—Na51^{xviii}	49.53 (13)	Na51—O6—Na5	30.7 (4)
O6^{i}—Na4—Na51^{xviii}	67.9 (3)	Si1—O6—Na52	91.6 (2)
O6^{xv}—Na4—Na51^{xviii}	112.2 (3)	Fe1—O6—Na52	100.22 (15)
O4^{xvi}—Na4—Na51^{xviii}	63.4 (2)	Na4^{ii}—O6—Na52	128.8 (4)
O4^{xvii}—Na4—Na51^{xviii}	101.6 (2)	Na51—O6—Na52	12.3 (3)
Na51^{iv}—Na4—Na51^{xviii}	159.6 (3)	Na5—O6—Na52	42.9 (4)
O2—Na4—Na52^{iv}	51.37 (15)	Si1—O6—Na53	85 (2)
O2^{iii}—Na4—Na52^{iv}	146.93 (19)	Fe1—O6—Na53	99.8 (18)
O6^{i}—Na4—Na52^{iv}	101.8 (3)	Na4^{ii}—O6—Na53	143 (3)
O6^{xv}—Na4—Na52^{iv}	78.4 (3)	Na51—O6—Na53	27 (3)
O4^{xvi}—Na4—Na52^{iv}	108.5 (2)	Na5—O6—Na53	58 (3)
O4^{xvii}—Na4—Na52^{iv}	56.4 (2)	Na52—O6—Na53	15 (3)
Na51^{iv}—Na4—Na52^{iv}	10.5 (2)		

Symmetry codes: (i) $-x+4/3, -x+y+2/3, -z+1/6$; (ii) $-y+2/3, x-y-2/3, z+1/3$; (iii) $y+2/3, x-2/3, -z-1/6$; (iv) $x-y, x-1, -z$; (v) $-y+1, -x+1, z+1/2$; (vi) $x-y, -y, -z-1/2$; (vii) $-x+2, -x+y+1, -z-1/2$; (viii) $y+1, x-1, -z-1/2$; (ix) $-y+1, x-y-1, z$; (x) $-x+y+2, -x+1, z$; (xi) $-x+2, -y, -z$; (xii) $y+1, -x+y+1, -z$; (xiii) $-x+y+2, y, z+1/2$; (xiv) $-y+1, -x+1, z-1/2$; (xv) $-x+y+4/3, -x+2/3, z-1/3$; (xvi) $y+1/3, -x+y+2/3, -z-1/3$; (xvii) $-x+y+4/3, y-1/3, z+1/6$; (xviii) $x-1/3, x-y-2/3, z-1/6$; (xix) $-x+5/3, -y+1/3, -z+1/3$; (xx) $x-y+1/3, x-1/3, -z-1/3$.